

Prise en compte de la topographie dans un modèle de Saint Venant à deux vitesses: solutions stationnaires et schémas numériques

Nelly BOULOS AL MAKARY



14 Mars 2023

Motivation



Figure – Floods in Haute-Garonne and Ariège, France 2022



Figure – Sediment transport and Deposition of the Rhone River

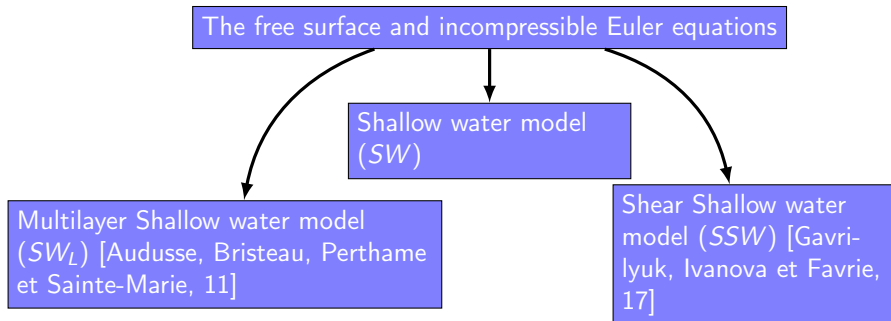
Motivation

The free surface and incompressible Euler equations

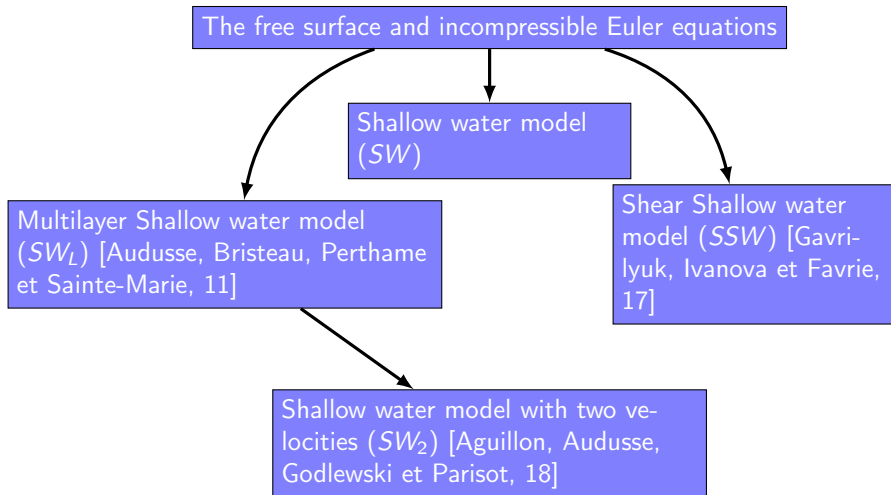


Shallow water model
(SW)

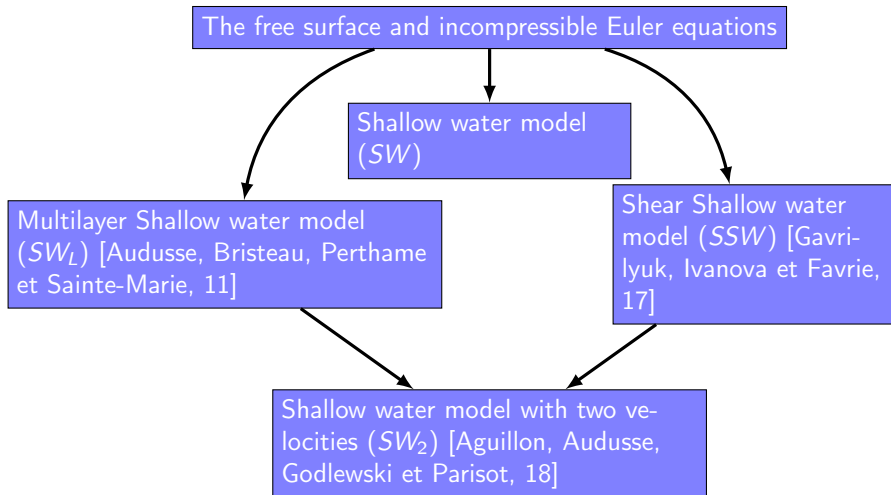
Motivation



Motivation



Motivation



The Shallow water model with two velocities

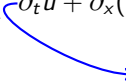
$$\begin{cases} \partial_t h + \partial_x(h\bar{u}) &= 0 \\ \partial_t(h\bar{u}) + \partial_x(h(\bar{u}^2 + \hat{u}^2) + \frac{g}{2}h^2) &= 0 \\ \partial_t \hat{u} + \partial_x(\bar{u}\hat{u}) &= 0 \end{cases} \quad (SW_2)$$

- $h(t, x) \in \mathbb{R}_+$ the water height
- $\bar{u}(t, x) \in \mathbb{R}$ the vertical-averaged of the horizontal velocity
- $\hat{u}(t, x) \in \mathbb{R}$ the signed standard deviation of the horizontal velocity

The Shallow water model with two velocities

$$\begin{cases} \partial_t h + \partial_x(h\bar{u}) &= 0 \\ \partial_t(h\bar{u}) + \partial_x(h(\bar{u}^2 + \hat{u}^2) + \frac{g}{2}h^2) &= 0 \\ \partial_t \hat{u} + \partial_x(\bar{u}\hat{u}) &= 0 \end{cases} \quad (SW_2)$$

For $\hat{u} = hS$,


$$\partial_t(hS) + \partial_x(\bar{u}hS) = 0$$

For $h > 0$,

$$\partial_t S + \bar{u}\partial_x S = 0$$

- $h(t, x) \in \mathbb{R}_+$ the water height
- $\bar{u}(t, x) \in \mathbb{R}$ the vertical-averaged of the horizontal velocity
- $\hat{u}(t, x) \in \mathbb{R}$ the signed standard deviation of the horizontal velocity

The Shallow water model with two velocities

$$\begin{cases} \partial_t h + \partial_x(h\bar{u}) &= 0 \\ \partial_t(h\bar{u}) + \partial_x(h(\bar{u}^2 + \hat{u}^2) + \frac{g}{2}h^2) &= -gh\partial_x Z \\ \partial_t \hat{u} + \partial_x(\bar{u}\hat{u}) &= 0 \end{cases} \quad (SW_2)$$

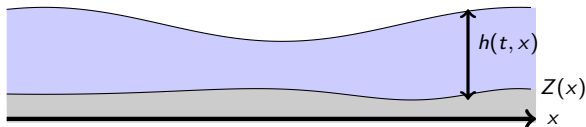
For $\hat{u} = hS$,

$$\partial_t(hS) + \partial_x(\bar{u}hS) = 0$$

For $h > 0$,

$$\partial_t S + \bar{u}\partial_x S = 0$$

- $h(t, x) \in \mathbb{R}_+$ the water height
- $\bar{u}(t, x) \in \mathbb{R}$ the vertical-averaged of the horizontal velocity
- $\hat{u}(t, x) \in \mathbb{R}$ the signed standard deviation of the horizontal velocity
- g the gravity
- $Z(x)$ the topography



The Shallow water model with two velocities

$$\begin{cases} \partial_t h + \partial_x(h\bar{u}) &= 0 \\ \partial_t(h\bar{u}) + \partial_x(h(\bar{u}^2 + \hat{u}^2) + \frac{g}{2}h^2) &= -gh\partial_x Z \\ \partial_t \hat{u} + \partial_x(\bar{u}\hat{u}) &= 0 \end{cases} \quad (SW_2)$$

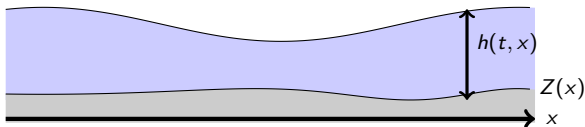
For $\hat{u} = hS$,

$$\partial_t(hS) + \partial_x(\bar{u}hS) = 0$$

For $h > 0$,

$$\partial_t S + \bar{u}\partial_x S = 0$$

- $h(t, x) \in \mathbb{R}_+$ the water height
- $\bar{u}(t, x) \in \mathbb{R}$ the vertical-averaged of the horizontal velocity
- $\hat{u}(t, x) \in \mathbb{R}$ the signed standard deviation of the horizontal velocity
- g the gravity
- $Z(x)$ the topography



⚠ For $\hat{u} = 0$, we retrieve the classical shallow water model.

Properties of the model

Mechanical energy

The mechanical energy reads

$$E = g \frac{h^2}{2} + \frac{h}{2} (\bar{u}^2 + \hat{u}^2),$$

and the associated energy flux is

$$G = \left(gh + \frac{\bar{u}^2 + 3\hat{u}^2}{2} \right) h\bar{u}.$$

The smooth solutions satisfy the energy conservation law

$$\partial_t E + \partial_x G = 0$$

whereas discontinuous solutions are selected to satisfy the following energy inequality condition

$$\partial_t E + \partial_x G \leq 0.$$

⚠ E is a convex function of $(h, h\bar{u}, h\hat{u})$ and not $(h, h\bar{u}, \hat{u})$.

Properties of the model

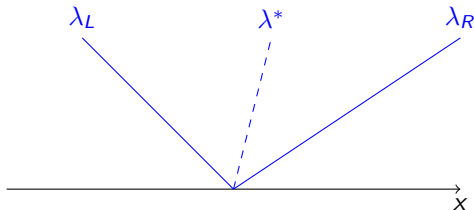
Hyperbolicity

We consider the set of variables

$$U = (h, h\bar{u}, \hat{u})$$

The eigenvalues are given by

$$\begin{cases} \lambda_L &= \bar{u} - \sqrt{gh + 3\hat{u}^2} \\ \lambda^* &= \bar{u}, \\ \lambda_R &= \bar{u} + \sqrt{gh + 3\hat{u}^2}, \end{cases}$$



- \bar{u} and $h\hat{u}^2 + \frac{g}{2}h^2$ are continuous through the λ^* -wave
- $\frac{\hat{u}}{h}$ is continuous through the external waves λ_L and λ_R (even through the shock)

Content

1 Steady State Solutions

2 Numerical schemes

3 Numerical results

Steady State solutions of the model with topography

$$\begin{cases} \partial_t h + \partial_x (h\bar{u}) &= 0, \\ \partial_t (h\bar{u}) + \partial_x (h(\bar{u}^2 + \hat{u}^2) + \frac{g}{2}h^2) &= -gh\partial_x Z, \\ \partial_t \hat{u} + \partial_x (\bar{u}\hat{u}) &= 0. \end{cases} \quad (SW_2)$$

We are interested in steady state solution in a bounded domain $x \in I = [x_L, x_R]$ defined from its boundary condition.

Hypothesis

We assume that there exists a point $x_0 \in I$ such that Z is a C^1 regular function, increasing on $[x_L, x_0]$ and decreasing on $[x_0, x_R]$.

The Froude number :

$$F_r := \frac{|\bar{u}|}{\sqrt{gh + 3\hat{u}^2}},$$

The flow is

$$\begin{cases} \textit{subcritical} & \text{if } F_r < 1, \\ \textit{critical} & \text{if } F_r = 1, \\ \textit{supercritical} & \text{if } F_r > 1, \end{cases}$$

Moving steady state solution

When the solution is C^1

$$\begin{cases} \partial_x (h\bar{u}) &= 0, \\ \partial_x \left(h(\bar{u}^2 + \hat{u}^2) + \frac{g}{2} h^2 \right) &= -gh\partial_x Z, \\ \partial_x (\bar{u}\hat{u}) &= 0. \end{cases}$$

Hence, the three quantities

- $h\bar{u}$
- $h + Z + \frac{1}{2g} (\bar{u}^2 + 3\hat{u}^2)$
- $\bar{u}\hat{u}$

are constant.

Moving steady state solution

When the solution is C^1

$$\begin{cases} \partial_x (h\bar{u}) &= 0, \\ \partial_x \left(h(\bar{u}^2 + \hat{u}^2) + \frac{g}{2} h^2 \right) &= -gh\partial_x Z, \\ \partial_x (\bar{u}\hat{u}) &= 0. \end{cases}$$

Hence, the three quantities

- $h\bar{u}$
- $h + Z + \frac{1}{2g} (\bar{u}^2 + 3\hat{u}^2)$
- $\bar{u}\hat{u}$

are constant.

At a point of discontinuity

The Rankine-Hugoniot jump conditions :

$$\begin{cases} [h\bar{u}] &= 0 \\ \left[h(\bar{u}^2 + \hat{u}^2) + \frac{g}{2} h^2 \right] &= 0 \\ [\bar{u}\hat{u}] &= 0, \end{cases}$$

The dissipation of entropy :

$$\left[\left(g(h + Z) + \frac{\bar{u}^2 + 3\hat{u}^2}{2} \right) h\bar{u} \right] \leq 0,$$

where $[X] = X^+ - X^-$.

Moving steady state solution

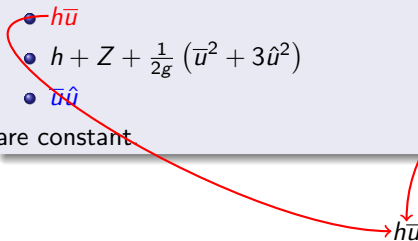
When the solution is C^1

$$\begin{cases} \partial_x (h\bar{u}) = 0, \\ \partial_x \left(h(\bar{u}^2 + \hat{u}^2) + \frac{g}{2} h^2 \right) = -gh\partial_x Z, \\ \partial_x (\bar{u}\hat{u}) = 0. \end{cases}$$

Hence, the three quantities

- $h\bar{u}$
- $h + Z + \frac{1}{2g} (\bar{u}^2 + 3\hat{u}^2)$
- $\bar{u}\hat{u}$

are constant


$$h\bar{u} = M$$

At a point of discontinuity

The Rankine-Hugoniot jump conditions :

$$\begin{cases} [h\bar{u}] = 0 \\ \left[h(\bar{u}^2 + \hat{u}^2) + \frac{g}{2} h^2 \right] = 0 \\ [\bar{u}\hat{u}] = 0, \end{cases}$$

The dissipation of entropy :

$$\left[\left(g(h + Z) + \frac{\bar{u}^2 + 3\hat{u}^2}{2} \right) h\bar{u} \right] \leq 0,$$

where $[X] = X^+ - X^-$.

Moving steady state solution

When the solution is C^1

$$\begin{cases} \partial_x (h\bar{u}) &= 0, \\ \partial_x \left(h(\bar{u}^2 + \hat{u}^2) + \frac{g}{2} h^2 \right) &= -gh\partial_x Z, \\ \partial_x (\bar{u}\hat{u}) &= 0. \end{cases}$$

Hence, the three quantities

$h\bar{u}$
 $h + Z + \frac{1}{2g} (\bar{u}^2 + 3\hat{u}^2)$
 $\bar{u}\hat{u}$
are constant

For $\bar{u} \neq 0$ and $h > 0$,

$$h\bar{u} = M$$

$$\frac{\hat{u}}{h} = S$$

At a point of discontinuity

The Rankine-Hugoniot jump conditions :

$$\begin{cases} [h\bar{u}] &= 0 \\ [h(\bar{u}^2 + \hat{u}^2) + \frac{g}{2} h^2] &= 0 \\ [\bar{u}\hat{u}] &= 0, \end{cases}$$

The dissipation of entropy :

$$\left[\left(g(h + Z) + \frac{\bar{u}^2 + 3\hat{u}^2}{2} \right) h\bar{u} \right] \leq 0,$$

where $[X] = X^+ - X^-$.

Moving steady state solutions

We fix $M > 0$ and $S \in \mathbb{R}$.

The Froude number rewrites

$$F_r = \frac{M}{h\sqrt{gh + 3S^2h^2}}.$$

We define the critical water height h_c corresponding to $F_r = 1$. Hence,

$$3S^2h_c^4 + gh_c^3 - M^2 = 0$$

The flow is supercritical if $h < h_c$, critical if $h = h_c$ and subcritical if $h > h_c$.

Proposition

For a given $M \in \mathbb{R}_+^*$, $S \in \mathbb{R}$, we define the function Φ as

$$\begin{aligned} \Phi &: \mathbb{R}_+^* \times \mathbb{R} \rightarrow \mathbb{R}_+^* \\ (h, Z) &\mapsto h + Z + \frac{1}{2g} \left(\frac{M^2}{h^2} + 3h^2 S^2 \right) \end{aligned}$$

Then, the function $x \mapsto h(x)$ is a C^1 steady state solution of (SW_2) if and only if there exists $K \in \mathbb{R}$ such that

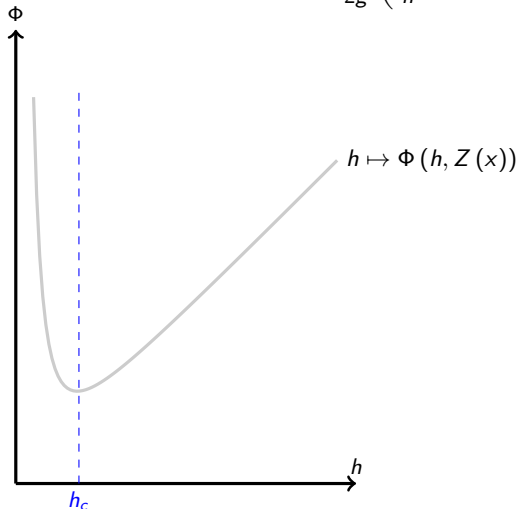
$$\forall x \in I, \Phi(h(x), Z(x)) = K$$

which is nothing more than the Bernoulli's principle in our context.

Regular moving steady state solutions

To define a C^1 solution on the interval I , we need to find for any $x \in I$ a solution $h(x)$ of the equation

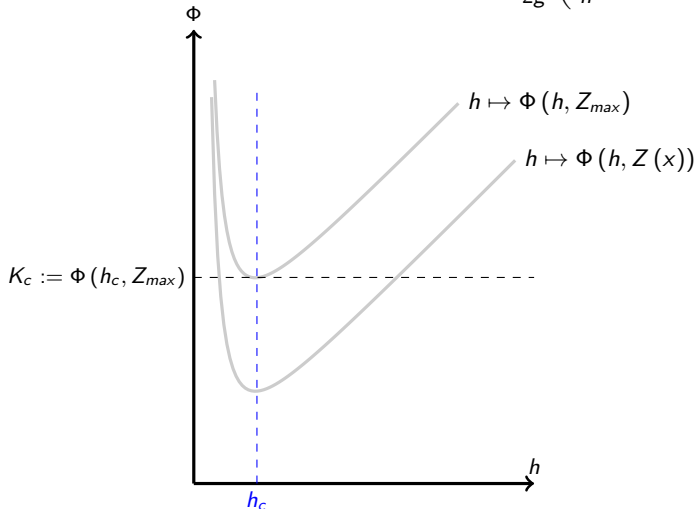
$$\Phi(h(x), Z(x)) = K \quad \text{where} \quad \Phi(h, Z) = h + Z + \frac{1}{2g} \left(\frac{M^2}{h^2} + 3h^2 S^2 \right).$$



Regular moving steady state solutions

To define a C^1 solution on the interval I , we need to find for any $x \in I$ a solution $h(x)$ of the equation

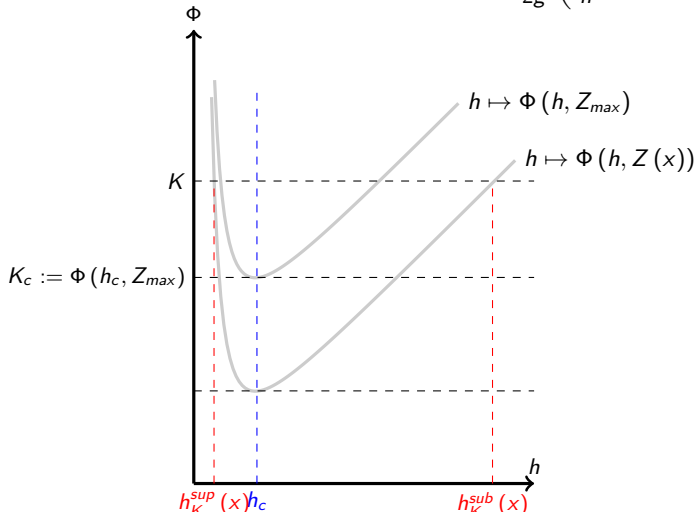
$$\Phi(h(x), Z(x)) = K \quad \text{where} \quad \Phi(h, Z) = h + Z + \frac{1}{2g} \left(\frac{M^2}{h^2} + 3h^2 S^2 \right).$$



Regular moving steady state solutions

To define a C^1 solution on the interval I , we need to find for any $x \in I$ a solution $h(x)$ of the equation

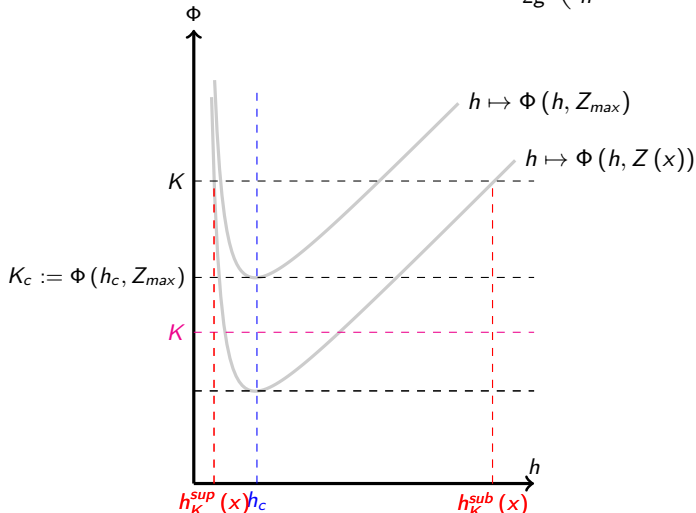
$$\Phi(h(x), Z(x)) = K \quad \text{where} \quad \Phi(h, Z) = h + Z + \frac{1}{2g} \left(\frac{M^2}{h^2} + 3h^2 S^2 \right).$$



Regular moving steady state solutions

To define a C^1 solution on the interval I , we need to find for any $x \in I$ a solution $h(x)$ of the equation

$$\Phi(h(x), Z(x)) = K \quad \text{where} \quad \Phi(h, Z) = h + Z + \frac{1}{2g} \left(\frac{M^2}{h^2} + 3h^2 S^2 \right).$$

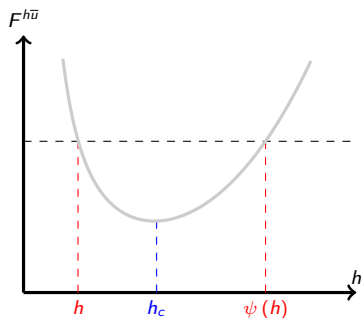


Stationary shocks and the entropy condition

Definition

For a given $M \in \mathbb{R}_+^*$, $S \in \mathbb{R}$, we define the function $F^{h\bar{u}}$ representing the momentum flux as

$$\begin{array}{rcl} F^{h\bar{u}} & : & \mathbb{R}_+^* \rightarrow \mathbb{R}_+^* \\ h & \mapsto & \frac{M^2}{h} + h^3 S^2 + \frac{g}{2} h^2. \end{array}$$

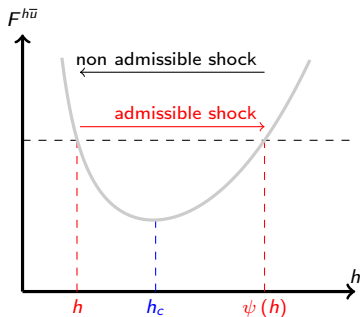


Stationary shocks and the entropy condition

Definition

For a given $M \in \mathbb{R}_+^*$, $S \in \mathbb{R}$, we define the function $F^{h\bar{u}}$ representing the momentum flux as

$$\begin{aligned} F^{h\bar{u}} : \mathbb{R}_+^* &\rightarrow \mathbb{R}_+^* \\ h &\mapsto \frac{M^2}{h} + h^3 S^2 + \frac{g}{2} h^2. \end{aligned}$$



Proposition

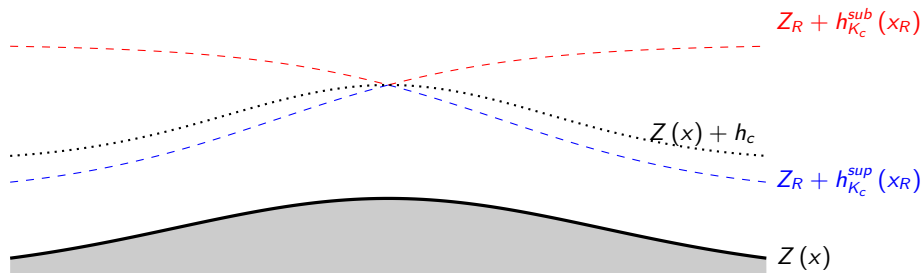
For a given $M \in \mathbb{R}_+^*$ and $S \in \mathbb{R}$, we suppose that $h^- \in \mathbb{R}_+^*$ and $\psi(h^-) = h^+$ are respectively the water heights at the left and at the right of a stationary shock. Then, the shock verifies the energy dissipation if one of the equivalent conditions below holds :

$$K^+ = \Phi(h^+, Z) \leq K^- = \Phi(h^-, Z)$$

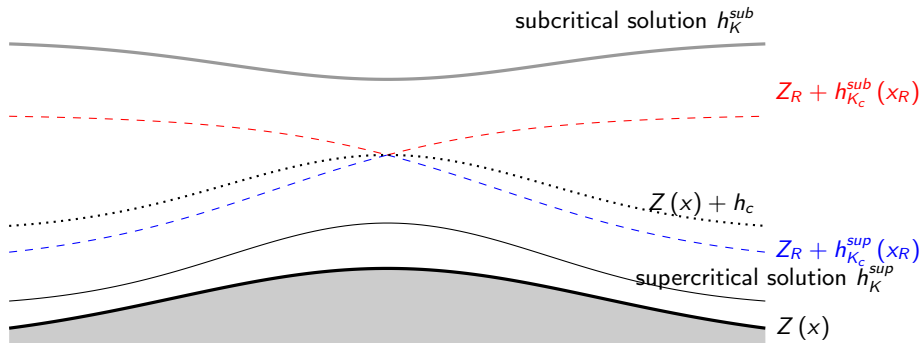
or

$$h^- < h_c < h^+.$$

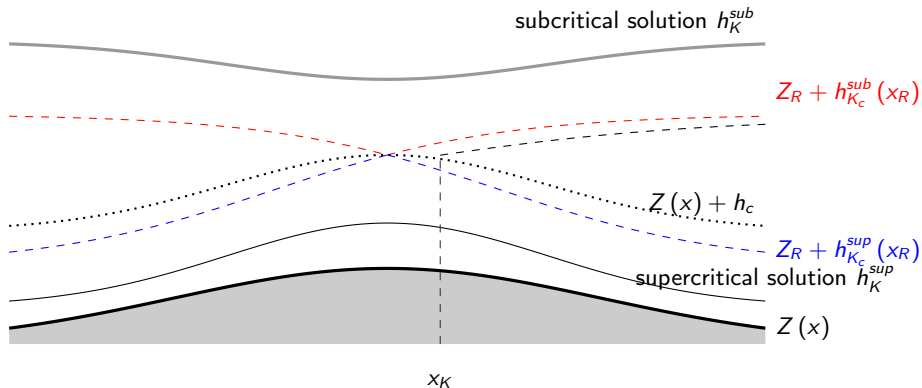
Moving steady state solutions



Moving steady state solutions



Moving steady state solutions



Representation of the eigenvalues for the different boundary conditions

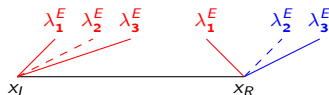
$$\lambda_1^E = \bar{u} - \sqrt{gh + 3\hat{u}^2}, \quad \lambda_2^E = \bar{u} \quad \text{and} \quad \lambda_3^E = \bar{u} + \sqrt{gh + 3\hat{u}^2}.$$



(a) Subcritical inlet and outlet boundaries



(b) Subcritical inlet and supercritical outlet boundaries



(c) Supercritical inlet and subcritical outlet boundaries



(d) Supercritical inlet and supercritical outlet boundaries

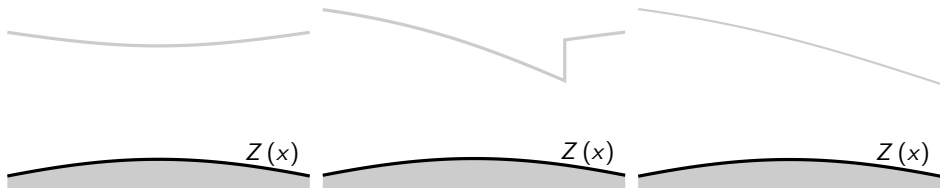
General steady state solutions for SW

Solutions with subcritical inlet boundary conditions [Swashes, 13]

$$M = 4.42m^2/s, h(x_R) = 2m$$

$$M = 0.18m^2/s, h(x_R) = 0.33m$$

$$M = 1.53m^2/s, h(x_R) = 0.66m$$



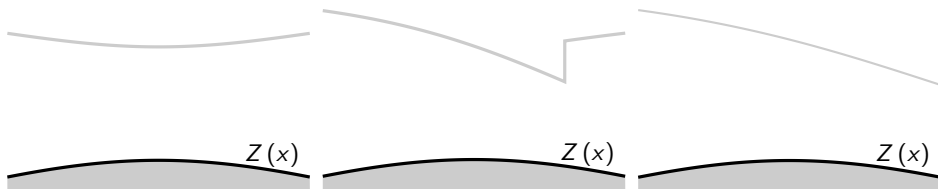
General steady state solutions for SW

Solutions with subcritical inlet boundary conditions [Swashes, 13]

$$M = 4.42\text{m}^2/\text{s}, h(x_R) = 2\text{m}$$

$$M = 0.18\text{m}^2/\text{s}, h(x_R) = 0.33\text{m}$$

$$M = 1.53\text{m}^2/\text{s}, h(x_R) = 0.66\text{m}$$



- What is the type of the solution for any parameter M and h ?
- Is there another type of solution verifying the same boundary conditions?
- What is the type of the solution when we add S ?

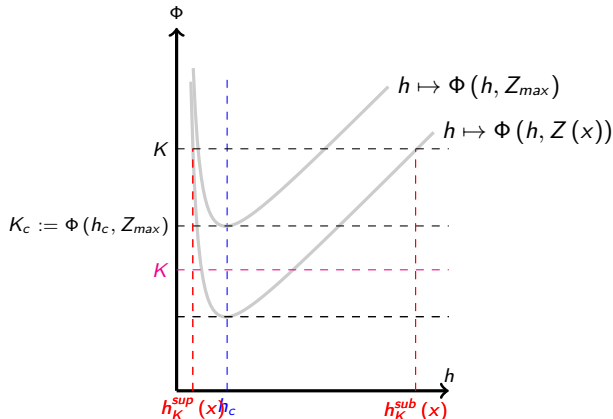
Construction of the stationary solutions

We fix $M > 0$ and $S \in \mathbb{R}$ then, we can compute h_c , K_c , $h_{K_c}^{sub}$ and $h_{K_c}^{sup}$.

With $h_L = h(x_L)$ and $h_R = h(x_R)$ we can compute

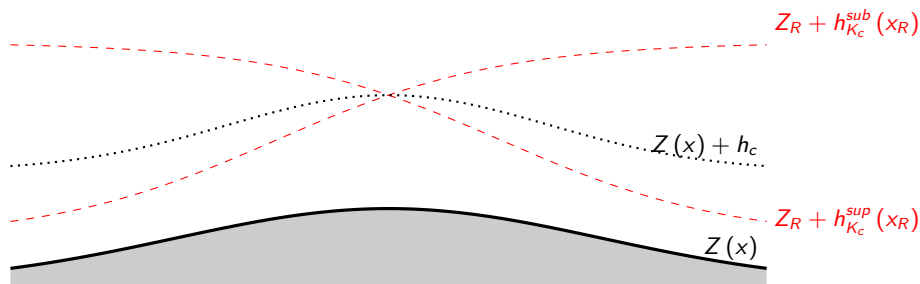
$$K_L = \Phi(h_L, Z_L), \quad \text{and} \quad K_R = \Phi(h_R, Z_R).$$

- 1 If a piecewise C^1 solution exists on I , then $K_L \geq K_c$ and $K_L \geq K_R$
- 2 The transition from the subcritical to the supercritical is continuous and occurs only at the top of the topography $x = x_0$ and with a critical hydraulic head K_c .
- 3 The solution may contain at most one shock on each side of the domain.



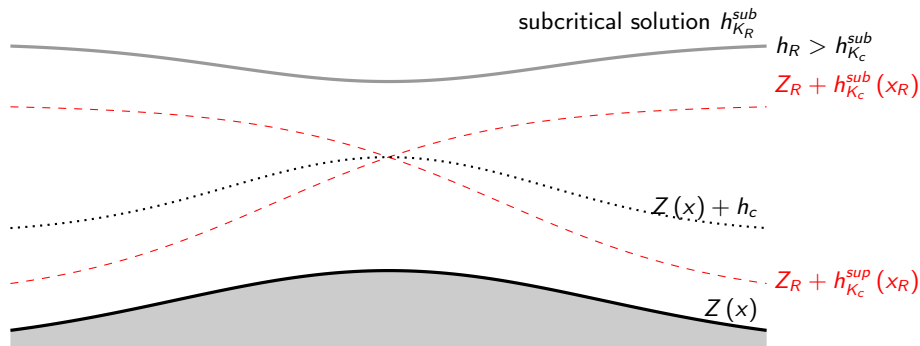
General steady states with subcritical boundary conditions at both sides of the domain

We fix one boundary condition of the form $h(x_R) = h_R$ and we suppose that $h(x_L) > h_c$



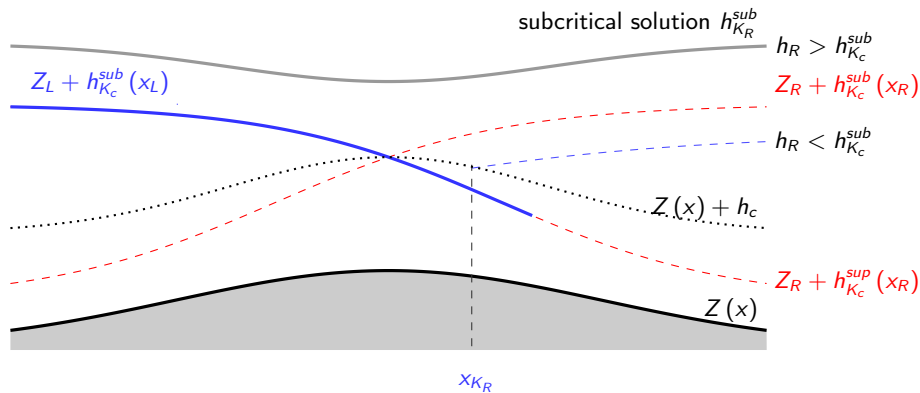
General steady states with subcritical boundary conditions at both sides of the domain

We fix one boundary condition of the form $h(x_R) = h_R$ and we suppose that $h(x_L) > h_c$



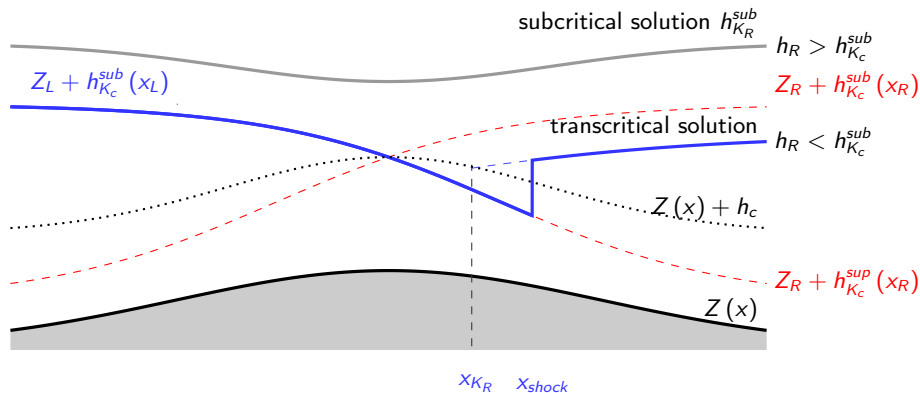
General steady states with subcritical boundary conditions at both sides of the domain

We fix one boundary condition of the form $h(x_R) = h_R$ and we suppose that $h(x_L) > h_c$



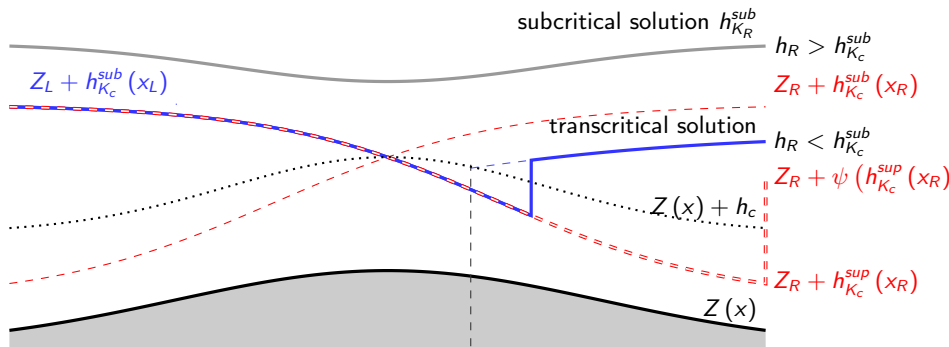
General steady states with subcritical boundary conditions at both sides of the domain

We fix one boundary condition of the form $h(x_R) = h_R$ and we suppose that $h(x_L) > h_c$



General steady states with subcritical boundary conditions at both sides of the domain

We fix one boundary condition of the form $h(x_R) = h_R$ and we suppose that $h(x_L) > h_c$



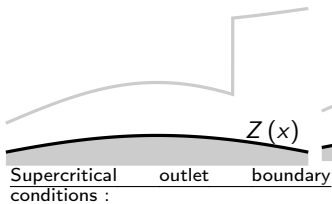
$$f : \begin{matrix} [x_{K_R}, x_R] \\ x \end{matrix} \rightarrow \mathbb{R} \quad \begin{matrix} x_{K_R} & x_{shock} \\ \bullet & \bullet \\ f(x_{K_R}) < 0 \\ f(x_R) > 0 \\ f \text{ is strictly increasing on } [x_{K_R}, x_R] \end{matrix}$$

$$x \mapsto F^{\bar{h}u}(h_{K_R}^{sub}(x)) - F^{\bar{h}u}(h_{K_c}^{sup}(x))$$

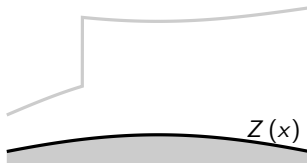
General steady states with supercritical inlet boundary conditions

Subcritical outlet boundary conditions :

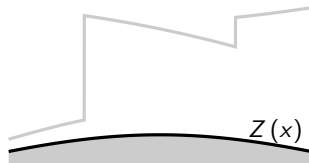
one shock at right



one shock at left



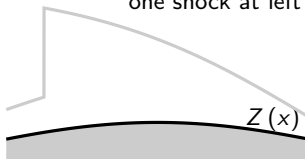
two shocks



supercritical everywhere



one shock at left



A formal analysis was done by physicists to prove that the shock at left is linearly non stable in [Baines et Whitehead, 03].

Uniqueness

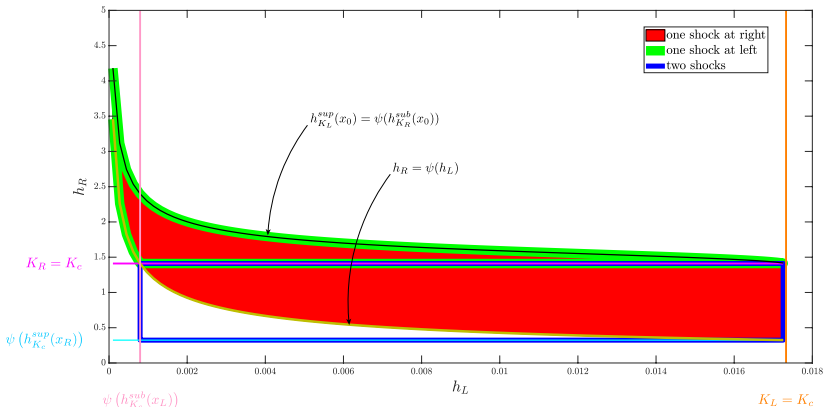


Figure – Sketch of the different zones of solutions with supercritical boundary condition at the left and subcritical boundary condition at the right for $M = 0.1$, $S = 1$, $g = 9.81$ and $Z(x_L) = Z(x_R)$.

Content

1 Steady State Solutions

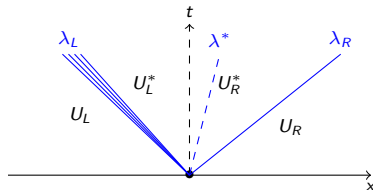
2 Numerical schemes

3 Numerical results

Description of the Godunov-type schemes

Godunov observed that U_i^n define at each cell interface $x_{i+\frac{1}{2}}$ a Riemann problem

$$\left\{ \begin{array}{l} \partial_t U + \partial_x F(U) = 0 \\ U(t^n, x) = \begin{cases} U_L & \text{if } x < x_{i+\frac{1}{2}} \\ U_R & \text{if } x \geq x_{i+\frac{1}{2}} \end{cases} \end{array} \right.$$

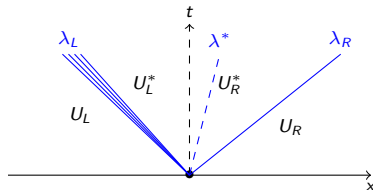


⚠ Computing the exact solution of the Riemann problem at each interface and for each time step is costly since it implies a fix point algorithm, see [Aguillon, Audusse, Godlewski et Pariset, 18]

Description of the Godunov-type schemes

Godunov observed that U_i^n define at each cell interface $x_{i+\frac{1}{2}}$ a Riemann problem

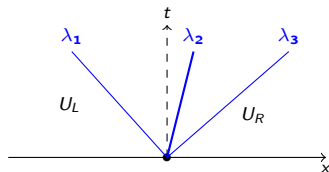
$$\begin{cases} \partial_t U + \partial_x F(U) = 0 \\ U(t^n, x) = \begin{cases} U_L & \text{if } x < x_{i+\frac{1}{2}} \\ U_R & \text{if } x \geq x_{i+\frac{1}{2}} \end{cases} \end{cases}$$



⚠ Computing the exact solution of the Riemann problem at each interface and for each time step is costly since it implies a fix point algorithm, see [Aguillon, Audusse, Godlewski et Parisot, 18]

The considered approximated Riemann solvers are

$$\tilde{U}\left(\frac{x}{t}, U_L, U_R\right) = \begin{cases} U_L = U_{\frac{1}{2}} & \text{if } \frac{x}{t} < \lambda_1, \\ \tilde{U}_{j+\frac{1}{2}} & \text{if } \lambda_j < \frac{x}{t} < \lambda_{j+1}, \\ U_R = U_{N+\frac{1}{2}} & \text{if } \frac{x}{t} > \lambda_N. \end{cases}$$



Description of the Godunov-type schemes

- 1 The external waves of the approximated solution have to be faster than the external wave speed of the exact solution

$$\lambda_L = \min(\bar{u}_L - c_L, \bar{u}_R - c_R), \\ \lambda_R = \max(\bar{u}_L + c_L, \bar{u}_R + c_R),$$

where $c_X = \sqrt{gh_X + 3\hat{u}_X^2}$.

- 2 The time step has to satisfy the following CFL condition

$$(\max_{j,i} |\lambda_{j,i+\frac{1}{2}}^n|) \Delta t^n \leq \frac{\Delta x}{2},$$

where $\lambda_{j,i+\frac{1}{2}}^n = \lambda_j(U_i^n, U_{i+1}^n)$.

- 3 The scheme has to satisfy a consistency property in the sense Harten and Lax showed in [Lax et al, 83]

$$\frac{1}{\Delta x} \int_{-\frac{\Delta x}{2}}^{\frac{\Delta x}{2}} \tilde{U}\left(\frac{x}{\Delta t^n}, U_L, U_R\right) dx = \frac{1}{\Delta x} \int_{-\frac{\Delta x}{2}}^{\frac{\Delta x}{2}} U_r\left(\frac{x}{\Delta t^n}, U_L, U_R\right) dx,$$

The $HLL_{\bar{u}}$ approximate Riemann solver

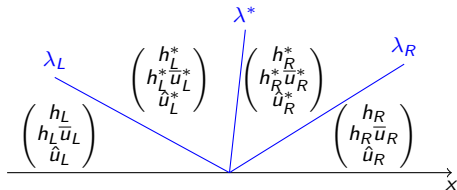
To determine the seven unknowns $(h_L^*, \bar{u}_L^*, \hat{u}_L^*)$, $(h_R^*, \bar{u}_R^*, \hat{u}_R^*)$ and λ^*

- we consider the consistency relations (3 equations)
- we impose the continuity of \bar{u} through the λ^* -wave

$$\bar{u}_L^* = \bar{u}_R^* = \lambda^*.$$

- we impose the continuity of $\frac{\hat{u}}{h}$ on the external waves λ_L and λ_R

$$\frac{\hat{u}_L}{h_L} = \frac{\hat{u}_L^*}{h_L^*} \quad \text{and} \quad \frac{\hat{u}_R}{h_R} = \frac{\hat{u}_R^*}{h_R^*}.$$



The $HLL_{\bar{u}}$ approximate Riemann solver

To determine the seven unknowns $(h_L^*, \bar{u}_L^*, \hat{u}_L^*)$, $(h_R^*, \bar{u}_R^*, \hat{u}_R^*)$ and λ^*

- we consider the consistency relations (3 equations)
- we impose the continuity of \bar{u} through the λ^* -wave

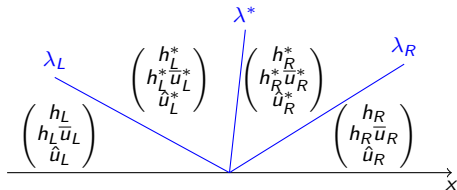
$$\bar{u}_L^* = \bar{u}_R^* = \lambda^*.$$

- we impose the continuity of $\frac{\hat{u}}{h}$ on the external waves λ_L and λ_R

$$\frac{\hat{u}_L}{h_L} = \frac{\hat{u}_L^*}{h_L^*} \quad \text{and} \quad \frac{\hat{u}_R}{h_R} = \frac{\hat{u}_R^*}{h_R^*}.$$

For $h_L > 0$ or $h_R > 0$, we are able to prove that

- $\lambda_L < \lambda^* = \bar{u}_{HLL} < \lambda_R$



$$\begin{cases} h_L^* = h_L \left(\frac{\lambda_L - \bar{u}_L}{\lambda_L - \bar{u}_{HLL}} \right), \\ h_R^* = h_R \left(\frac{\lambda_R - \bar{u}_R}{\lambda_R - \bar{u}_{HLL}} \right), \end{cases}$$

$$\text{with} \quad \bar{u}_{HLL} = \frac{[\lambda h \bar{u} - h(\bar{u}^2 + \hat{u}^2) - \frac{g}{2} h^2]}{[h(\lambda - \bar{u})]}.$$

The $HLL_{\bar{u}}$ approximate Riemann solver

To determine the seven unknowns $(h_L^*, \bar{u}_L^*, \hat{u}_L^*)$, $(h_R^*, \bar{u}_R^*, \hat{u}_R^*)$ and λ^*

- we consider the consistency relations (3 equations)
- we impose the continuity of \bar{u} through the λ^* -wave

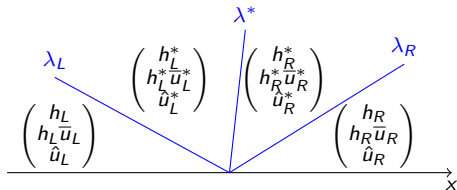
$$\bar{u}_L^* = \bar{u}_R^* = \lambda^*.$$

- we impose the continuity of $\frac{\hat{u}}{h}$ on the external waves λ_L and λ_R

$$\frac{\hat{u}_L}{h_L} = \frac{\hat{u}_L^*}{h_L^*} \quad \text{and} \quad \frac{\hat{u}_R}{h_R} = \frac{\hat{u}_R^*}{h_R^*}.$$

For $h_L > 0$ or $h_R > 0$, we are able to prove that

- $\lambda_L < \lambda^* = \bar{u}_{HLL} < \lambda_R$



$$\begin{cases} h_L^* = h_L \left(\frac{\lambda_L - \bar{u}_L}{\lambda_L - \bar{u}_{HLL}} \right), \\ h_R^* = h_R \left(\frac{\lambda_R - \bar{u}_R}{\lambda_R - \bar{u}_{HLL}} \right), \end{cases}$$

$$\text{with} \quad \bar{u}_{HLL} = \frac{[\lambda h \bar{u} - h(\bar{u}^2 + \hat{u}^2) - \frac{g}{2} h^2]}{[h(\lambda - \bar{u})]}.$$

⚠ The scheme is equivalent to the Siliciu scheme proposed in [Bouchut, 04] and the 3-waves ARS proposed by [Chandrashekar, Nkonga, Meena et Bhole, 20]

The $HLL_{\bar{u}}$ approximate Riemann solver

Properties of the scheme

- Preserves the positivity of the water heights.
- Satisfies the maximum principle on S .
- Satisfies the preservation of the stationary contact discontinuity where $\bar{u} = 0$ and $h\hat{u}^2 + \frac{g}{2}h^2$ is constant.
- Verifies a discrete energy inequality of the scheme?

If there exists a numerical energy flux $\mathcal{G}(U_L, U_R)$ which is consistent with the exact energy flux, i.e $\mathcal{G}(U, U) = G(U)$ such that

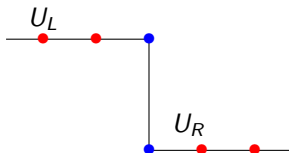
$$\forall i \in \mathbb{Z}, \forall n \in \mathbb{N}, \quad E(U_i^{n+1}) - E(U_i^n) + \frac{\Delta t^n}{\Delta x} \left(\mathcal{G}_{i+\frac{1}{2}}^n - \mathcal{G}_{i-\frac{1}{2}}^n \right) \leq 0, \quad (1)$$

where

$$\mathcal{G}_{i+\frac{1}{2}}^n = \mathcal{G}(U_{i+1}^n, U_i^n).$$

⚠ E is a convex function of $(h, h\bar{u}, h\hat{u})$ and not $(h, h\bar{u}, \hat{u})$

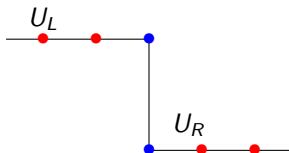
The $HLL_{\bar{u}}$ approximate Riemann solver



More precisely, if (1) is verified then, it is necessarily true in the two cells separating the discontinuity. In other words, for one time step, we have

$$\begin{cases} E(U_L^1) - E(U_L^0) + \frac{\Delta t^n}{\Delta x} \left(\mathcal{G}_{\frac{3}{2}}^0 - G(U_L^0) \right) \leq 0, \\ E(U_R^1) - E(U_R^0) + \frac{\Delta t^n}{\Delta x} \left(G(U_R^0) - \mathcal{G}_{\frac{3}{2}}^0 \right) \leq 0, \end{cases}$$

The $HLL_{\bar{u}}$ approximate Riemann solver



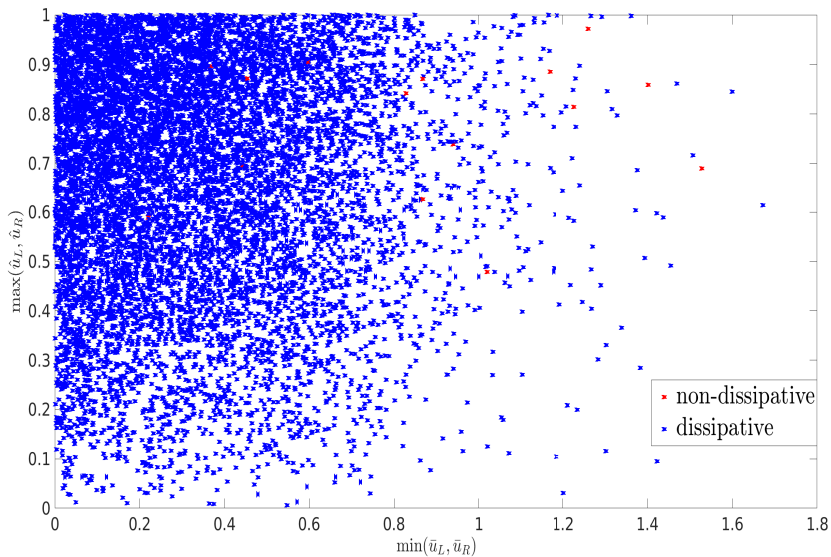
More precisely, if (1) is verified then, it is necessarily true in the two cells separating the discontinuity. In other words, for one time step, we have

$$\begin{cases} E(U_L^1) - E(U_L^0) + \frac{\Delta t^n}{\Delta x} \left(\mathcal{G}_{\frac{3}{2}}^0 - G(U_L^0) \right) \leq 0, \\ E(U_R^1) - E(U_R^0) + \frac{\Delta t^n}{\Delta x} \left(G(U_R^0) - \mathcal{G}_{\frac{3}{2}}^0 \right) \leq 0, \end{cases}$$

\Rightarrow

$$\Delta E^{0,1} := E(U_R^1) + E(U_L^1) - (E(U_R^0) + E(U_L^0)) + \frac{\Delta t^n}{\Delta x} (G(U_R^0) - G(U_L^0)) \leq 0. \quad (2)$$

Properties of the scheme



Numerical schemes for the model with topography

We consider now the set of variables

$$W = (h, h\bar{u}, \hat{u}, Z).$$

- Schemes that are accurate on the contact discontinuity while verifying a well-balanced property for all regular steady states of the system (SW_2).

Numerical schemes for the model with topography

We consider now the set of variables

$$W = (h, h\bar{u}, \hat{u}, Z).$$

- Schemes that are accurate on the contact discontinuity while verifying a well-balanced property for all regular steady states of the system (SW_2).

The C^1 steady states of (SW_2) system are governed by

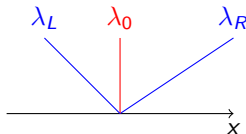
$$\begin{cases} \partial_x (h\bar{u}) = 0, \\ \partial_x (h(\bar{u}^2 + \hat{u}^2) + \frac{g}{2}h^2) = -gh\partial_x Z, \\ \partial_x (\bar{u}\hat{u}) = 0 \end{cases} \implies \begin{cases} h\bar{u} = M, \\ \frac{\bar{u}^2}{2} + \frac{3\hat{u}^2}{2} + g(h + Z) = K, \\ \bar{u}\hat{u} = MS. \end{cases}$$

For all $W_L = (h_L, h_L\bar{u}_L, \hat{u}_L, Z_L)$ and $W_R = (h_R, h_R\bar{u}_R, \hat{u}_R, Z_R)$ at steady state, the well balanced approximate Riemann solver \tilde{W} should verify

$$\tilde{W}\left(\frac{x}{t}, W_L, W_R\right) = \begin{cases} W_L & \text{if } \frac{x}{t} < 0, \\ W_R & \text{if } \frac{x}{t} > 0. \end{cases}$$

Numerical schemes for the model with topography

Now we have an additional wave which is the stationary wave λ_0 due to the presence of the topography



- 1 To preserve the order of the waves, we choose the following two external waves

$$\begin{aligned}\lambda_L &= \min(\bar{u}_L - c_L, \bar{u}_R - c_R, 0), \\ \lambda_R &= \max(\bar{u}_L + c_L, \bar{u}_R + c_R, 0),\end{aligned}$$

- 2 The consistency relation now reads

$$F(W_R) - F(W_L) - \Delta x \cdot \tilde{B}(\Delta x, \Delta t^n, W_L, W_R) = \sum_{j=1}^N \lambda_j \left(\tilde{W}_{j+\frac{1}{2}} - \tilde{W}_{j-\frac{1}{2}} \right).$$

where \tilde{B} is a numerical approximation of the source term verifying

$$\tilde{B}_{W_L, W_R \rightarrow W}^{\Delta x \rightarrow 0} \sim -gh\Delta Z.$$

Numerical schemes for the model with topography

Existing works

- [Berthon et Chalons, 16]
- [Michel-Dansac, Berthon, Clain et Foucher, 17]
- [Berthon, M'baye, Le et Seck, 21]

Numerical schemes for the model with topography

Existing works

- [Berthon et Chalons, 16]
- [Michel-Dansac, Berthon, Clain et Foucher, 17]
- [Berthon, M'baye, Le et Seck, 21]

Numerical schemes for the model with topography

Existing works

- [Berthon et Chalons, 16]
- [Michel-Dansac, Berthon, Clain et Foucher, 17]
- [Berthon, M'baye, Le et Seck, 21]
- [Berthon, Desveaux, Klingenberg et Zenk, 16]
- [Desveaux et Masset, 21]

Numerical schemes for the model with topography

Existing works

- [Berthon et Chalons, 16]
- [Michel-Dansac, Berthon, Clain et Foucher, 17]
- [Berthon, M'baye, Le et Seck, 21]
- [Berthon, Desveaux, Klingenberg et Zenk, 16]
- [Desveaux et Masset, 21]

Let us introduce the quantity (steady state indicator)

$$\epsilon_{L,R} = |K_R - K_L| + |M_R - M_L| + |S_R - S_L|.$$

The smooth steady state solutions of (SW_2) for a Riemann problem are then characterized by

$$\epsilon_{L,R} = 0.$$

Definition

Suppose that $h_L > 0$ and $h_R > 0$. We define

$$\overline{M^2} = |M_L M_R|, \quad \overline{S^2} = |S_L S_R|, \quad \bar{h} = \frac{h_L + h_R}{2}, \quad \tilde{F}_{\bar{h}, M, S} = \frac{\overline{M^2} \bar{h}}{g h_L^2 h_R^2} - 3 \frac{\overline{S^2} \bar{h}}{g}.$$

When $\tilde{F}_{\bar{h}, M, S} \neq 1$ or $\epsilon_{L,R} \neq 0$, let us define an approximation of the interface topography source term by

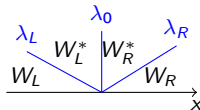
$$\Delta x \cdot \tilde{B}^M = -g \bar{h} (Z_R - Z_L) + \left(\frac{\overline{M^2}}{4 h_L^2 h_R^2} + \frac{\overline{S^2}}{4} \right) \frac{(h_R - h_L)(Z_R - Z_L)^2}{\left(1 - \tilde{F}_{\bar{h}, M, S}\right)^2 + \epsilon_{L,R}}.$$

- consistent with $-gh\partial_x Z$
- vanishes for a flat topography
- is adapted for the construction of well-balanced schemes.

The HLL_0 scheme

We introduce the following notation

$$A_{h_{HLL}\bar{u}_{HLL},\tilde{B}} = (\lambda_R - \lambda_L) h_{HLL} \bar{u}_{HLL} + \Delta x \cdot \tilde{B}.$$



The integral consistency relations imply

$$\begin{cases} \lambda_R h_R^* - \lambda_L h_L^* &= (\lambda_R - \lambda_L) h_{HLL}, \\ \lambda_R h_R^* \bar{u}_R^* - \lambda_L h_L^* \bar{u}_L^* &= A_{h_{HLL}\bar{u}_{HLL},\tilde{B}}, \\ \lambda_R \hat{u}_R^* - \lambda_L \hat{u}_L^* &= (\lambda_R - \lambda_L) \hat{u}_{HLL}, \end{cases}$$

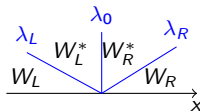
We consider that the states L^* and R^* verify through the contact discontinuity λ_0 , a discrete version of the smooth steady state solutions

$$\begin{cases} [h\bar{u}]_{L^*}^{R^*} &= 0, \\ [h(\bar{u}^2 + \hat{u}^2) + \frac{g}{2}h^2]_{L^*}^{R^*} &= \Delta x \cdot \tilde{B}, \\ [\hat{u}\bar{u}]_{L^*}^{R^*} &= 0 \end{cases}$$

The HLL_0 scheme

We introduce the following notation

$$A_{h_{HLL}\bar{u}_{HLL},\tilde{B}} = (\lambda_R - \lambda_L) h_{HLL} \bar{u}_{HLL} + \Delta x \cdot \tilde{B}.$$



The integral consistency relations imply

$$\begin{cases} \lambda_R h_R^* - \lambda_L h_L^* &= (\lambda_R - \lambda_L) h_{HLL}, \\ \lambda_R h_R^* \bar{u}_R^* - \lambda_L h_L^* \bar{u}_L^* &= A_{h_{HLL}\bar{u}_{HLL},\tilde{B}}, \\ \lambda_R \hat{u}_R^* - \lambda_L \hat{u}_L^* &= (\lambda_R - \lambda_L) \hat{u}_{HLL}, \end{cases}$$

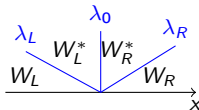
We consider that the states L^* and R^* verify through the contact discontinuity λ_0 , a discrete version of the smooth steady state solutions

$$\begin{cases} [h\bar{u}]_{L^*}^{R^*} &= 0, \\ [h(\bar{u}^2 + \hat{u}^2) + \frac{g}{2}h^2]_{L^*}^{R^*} &= \Delta x \cdot \tilde{B}, \\ [\hat{u}\bar{u}]_{L^*}^{R^*} &= 0 \end{cases} \implies \begin{cases} h_R^* \bar{u}_R^* = h_L^* \bar{u}_L^* := M^*, \\ \frac{\hat{u}_R^*}{h_R^*} = \frac{\hat{u}_L^*}{h_L^*} := S^*. \end{cases}$$

The HLL_0 scheme

We introduce the following notation

$$A_{h_{HLL}\bar{u}_{HLL},\tilde{B}} = (\lambda_R - \lambda_L) h_{HLL} \bar{u}_{HLL} + \Delta x \cdot \tilde{B}.$$



The integral consistency relations imply

$$\begin{cases} \lambda_R h_R^* - \lambda_L h_L^* = (\lambda_R - \lambda_L) h_{HLL}, \\ \lambda_R h_R^* \bar{u}_R^* - \lambda_L h_L^* \bar{u}_L^* = A_{h_{HLL}\bar{u}_{HLL},\tilde{B}}, \\ \lambda_R \hat{u}_R^* - \lambda_L \hat{u}_L^* = (\lambda_R - \lambda_L) \hat{u}_{HLL}, \end{cases}$$

We consider that the states L^* and R^* verify through the contact discontinuity λ_0 , a discrete version of the smooth steady state solutions

$$\begin{cases} [h\bar{u}]_{L^*}^{R^*} = 0, \\ [h(\bar{u}^2 + \hat{u}^2) + \frac{g}{2}h^2]_{L^*}^{R^*} = \Delta x \cdot \tilde{B}, \\ [\hat{u}\bar{u}]_{L^*}^{R^*} = 0 \end{cases} \implies \begin{cases} h_R^* \bar{u}_R^* = h_L^* \bar{u}_L^* := M^*, \\ M^{*2} [\frac{1}{h}]_{L^*}^{R^*} + S^{*2} [h^3]_{L^*}^{R^*} + \frac{g}{2} [h^2]_{L^*}^{R^*} = \Delta x \cdot \tilde{B}, \\ \frac{\hat{u}_R^*}{h_R^*} = \frac{\hat{u}_L^*}{h_L^*} := S^*. \end{cases}$$

Then, the sixth relation is

$$(h_R^* - h_L^*) = C_{\alpha_{L,R},\tilde{B}} \quad \text{with} \quad C_{\alpha_{L,R},\tilde{B}} := \frac{\alpha_{L,R} \Delta x \cdot \tilde{B}}{\alpha_{L,R}^2 + \epsilon_{L,R}}.$$

and

$$\alpha_{L,R} = \frac{-\overline{M^2}}{h_L h_R} + \frac{g}{2} (h_R + h_L) + \overline{S^2} (h_R^2 + h_L h_R + h_L^2).$$

The HLL_0 scheme

Well-balanced version of the HLL_0 scheme

For, $h_L > 0$ and $h_R > 0$, the HLL_0 scheme defined by

$$\left\{ \begin{array}{l} h_L^* = h_{HLL} - \frac{\lambda_R C_{\alpha_{L,R}, \tilde{B}}}{(\lambda_R - \lambda_L)}, \\ h_R^* = h_{HLL} - \frac{\lambda_L C_{\alpha_{L,R}, \tilde{B}}}{(\lambda_R - \lambda_L)}, \\ \bar{u}_L^* = \frac{h_{HLL} \bar{u}_{HLL} + \frac{\Delta x \cdot \tilde{B}}{\lambda_R - \lambda_L}}{h_L^*}, \\ \bar{u}_R^* = \frac{h_{HLL} \bar{u}_{HLL} + \frac{\Delta x \cdot \tilde{B}}{\lambda_R - \lambda_L}}{h_R^*}, \\ \hat{u}_L^* = \hat{u}_{HLL} \frac{h_L^*}{h_{HLL}}, \\ \hat{u}_R^* = \hat{u}_{HLL} \frac{h_R^*}{h_{HLL}}, \end{array} \right. \quad (HLL_0)$$

Proposition

Suppose that $\epsilon_{L,R} = 0$. Then, with the approximation of the source term defined earlier, we have

$$W_L^* = W_L \quad \text{and} \quad W_R^* = W_R$$

and the HLL_0 scheme is well-balanced

The HLL_0 scheme

Positive and well-balanced version of the HLL_0 scheme

Our strategy is to test the positivity of the quantities \tilde{h}_L^* and \tilde{h}_R^* defined by

$$\tilde{h}_L^* = h_{HLL} - \frac{\lambda_R C_{\alpha_L, R, \tilde{B}}}{(\lambda_R - \lambda_L)} \quad \text{and} \quad \tilde{h}_R^* = h_{HLL} - \frac{\lambda_L C_{\alpha_L, R, \tilde{B}}}{(\lambda_R - \lambda_L)}.$$

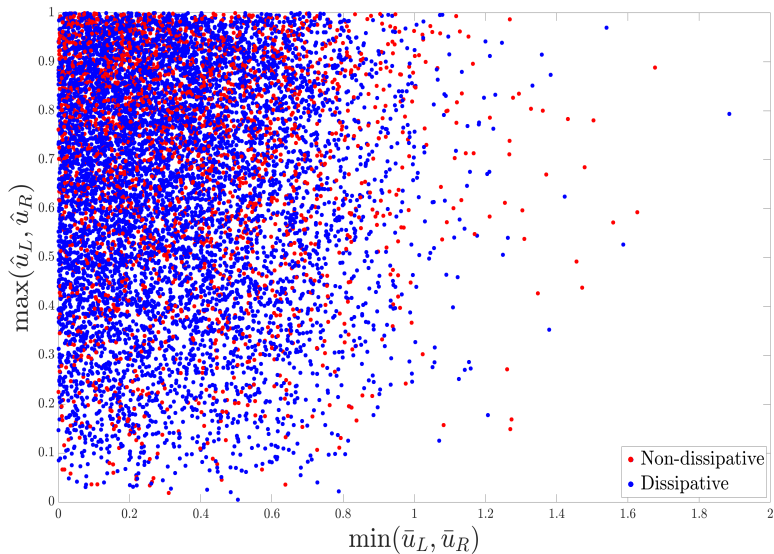
Then, the correction is interpreted as the solution of a new ARS with vanishing intermediate states.

- The case $\tilde{h}_L^* > 0$ and $\tilde{h}_R^* > 0$ then, the intermediate states defined in (HLL_0) .
- The case $\tilde{h}_L^* < 0$ and $\tilde{h}_R^* > 0$ then, the scheme is defined by
- The case $\tilde{h}_L^* > 0$ and $\tilde{h}_R^* < 0$ then, the scheme is defined by

$$\left\{ \begin{array}{l} h_L^* = 0, \\ h_R^* = \frac{(\lambda_R - \lambda_L) h_{HLL}}{\lambda_R}, \\ \bar{u}_L^* = 0, \\ \bar{u}_R^* = \frac{A_{h_{HLL} \bar{u}_{HLL}, \tilde{B}}}{\lambda_R \tilde{h}_R^*}, \\ \hat{u}_L^* = 0, \\ \hat{u}_R^* = \frac{(\lambda_R - \lambda_L) \hat{u}_{HLL}}{\lambda_R}, \end{array} \right.$$

$$\left\{ \begin{array}{l} h_L^* = -\frac{(\lambda_R - \lambda_L) h_{HLL}}{\lambda_L}, \\ h_R^* = 0, \\ \bar{u}_L^* = -\frac{A_{h_{HLL} \bar{u}_{HLL}, \tilde{B}}}{\lambda_L h_L^*}, \\ \bar{u}_R^* = 0, \\ \hat{u}_L^* = -\frac{(\lambda_R - \lambda_L) \hat{u}_{HLL}}{\lambda_L}, \\ \hat{u}_R^* = 0. \end{array} \right.$$

The HLL_0 scheme



The $HLL_{0,\bar{u}}$ scheme

Here we propose a second 4-waves ARS that is a mixture between HLL_0 and $HLL_{\bar{u}}$.

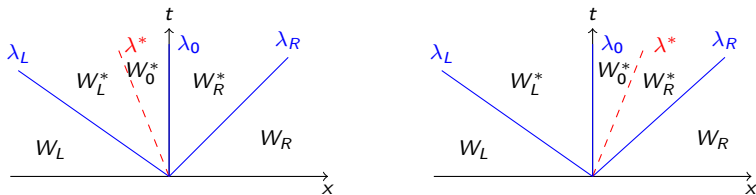


Figure – The waves representation of the $HLL_{0,\bar{u}}$ approximate Riemann solver with $\lambda^* < 0$ on the left and $\lambda^* > 0$ on the right.

The $HLL_{0,\bar{u}}$ scheme

- Similarly to $HLL_{\bar{u}}$, we impose the continuity \bar{u} across the transport wave.

$$\lambda^* = \begin{cases} \bar{u}_L^* = \bar{u}_0^* & \text{if } \lambda^* < 0, \\ \bar{u}_R^* = \bar{u}_0^* & \text{if } \lambda^* > 0. \end{cases}$$

- Similarly to HLL_0 , we consider the Riemann invariant across the stationary wave

$$(h_0^* \bar{u}_0^*, \bar{u}_0^* \hat{u}_0^*) = \begin{cases} (h_R^* \bar{u}_R^*, \bar{u}_R^* \hat{u}_R^*) & \text{if } \lambda^* < 0, \\ (h_L^* \bar{u}_L^*, \bar{u}_L^* \hat{u}_L^*) & \text{if } \lambda^* > 0 \end{cases}$$

- We consider the consistency relation
- The linearization across the stationary wave implies

$$C_{\alpha_{L,R}, \tilde{B}} = \begin{cases} (h_R^* - h_0^*) & \text{if } \lambda^* < 0, \\ (h_0^* - h_L^*) & \text{if } \lambda^* > 0 \end{cases}$$

- We impose the continuity of $\frac{\hat{u}}{h}$ on the external waves λ_L and λ_R

$$\frac{\hat{u}_L}{h_L} = \frac{\hat{u}_L^*}{h_L^*} \quad \text{and} \quad \frac{\hat{u}_R}{h_R} = \frac{\hat{u}_R^*}{h_R^*}.$$

The $HLL_{0,\bar{u}}$ scheme

Proposition

Assume that h_L , h_R , h_L^ , h_0^* and h_R^* are positive. Suppose that $\lambda_L < \lambda^* < \lambda_R$ therefore, the sign of \bar{u}_L^* , \bar{u}_0^* , \bar{u}_R^* and λ^* is the same of the sign as $A_{h_{HLL}\bar{u}_{HLL},\tilde{B}}$.*

Well-balanced version of the $HLL_{0,\bar{u}}$ scheme

Assume that $h_L > 0$, $h_R > 0$ and $\lambda_L < \lambda^* < \lambda_R$. Assume that the previous proposition is verified. Then, the system admits a unique solution

$$(h_L^*, h_0^*, h_R^*, \bar{u}_L^*, \bar{u}_0^*, \bar{u}_R^*, \hat{u}_L^*, \hat{u}_0^*, \hat{u}_R^*, \lambda^*) \in \mathbb{R}^{10}.$$

For W_L and W_R defining a smooth steady state, if $h_L > 0$ and $h_R > 0$ then, the scheme satisfies the well-balanced property.

The $HLL_{0,\bar{u}}$ scheme

Proposition

Assume that h_L, h_R, h_L^*, h_0^* and h_R^* are positive. Suppose that $\lambda_L < \lambda^* < \lambda_R$ therefore, the sign of $\bar{u}_L^*, \bar{u}_0^*, \bar{u}_R^*$ and λ^* is the same of the sign as $A_{h_{HLL}\bar{u}_{HLL},\tilde{B}}$.

Well-balanced version of the $HLL_{0,\bar{u}}$ scheme

Assume that $h_L > 0, h_R > 0$ and $\lambda_L < \lambda^* < \lambda_R$. Assume that the previous proposition is verified. Then, the system admits a unique solution

$$(h_L^*, h_0^*, h_R^*, \bar{u}_L^*, \bar{u}_0^*, \bar{u}_R^*, \hat{u}_L^*, \hat{u}_0^*, \hat{u}_R^*, \lambda^*) \in \mathbb{R}^{10}.$$

For W_L and W_R defining a smooth steady state, if $h_L > 0$ and $h_R > 0$ then, the scheme satisfies the well-balanced property.

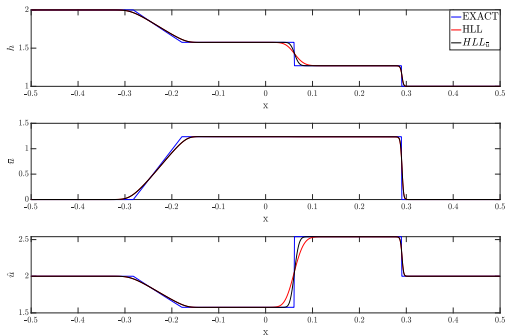
Content

1 Steady State Solutions

2 Numerical schemes

3 Numerical results

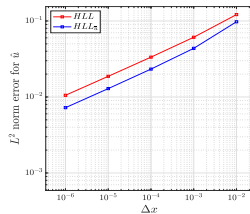
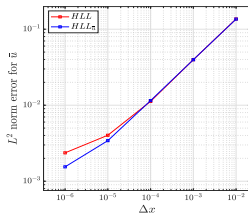
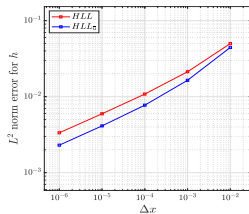
Dam break problem



$\mathcal{O}(\Delta x^{0.25})$

$\mathcal{O}(\Delta x^{0.35})$

$\mathcal{O}(\Delta x^{0.25})$



Numerical stability of the stationary solutions

Setting the parameters

- $I =]0, 25[$
- $Z(x) = \max\left(0, 0.2 - 0.05(x - x_0)^2\right),$
- $M = 1.2m/s$ and $S = 0.5m/s.$

Initial Conditions

- When the inlet boundary conditions are subcritical, the initial conditions satisfy the lake at rest , i.e

$$h + z = h_R, \quad M = 0 \quad \text{and} \quad S = 0.$$

- When the inlet boundary conditions are supercritical, the initial conditions are chosen to be the analytical solution.

Subcritical solution

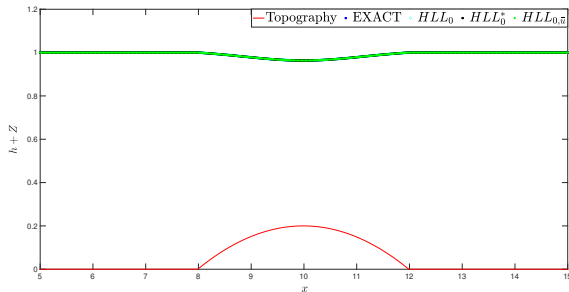


Figure – Free surface and topography for the subcritical solution

| | $h + Z$ | M | S |
|-------------------|-------------|--------------|-------------|
| HLL_0 | $5.6e - 14$ | $2.02e - 14$ | $2.7e - 14$ |
| HLL_0^* | $6e - 14$ | $1.7e - 14$ | $3.2e - 14$ |
| $HLL_{0,\bar{u}}$ | $5.4e - 14$ | $1.9e - 14$ | $3.2e - 14$ |

Table – Free surface, discharge and shear errors for the subcritical solution

Transcritical solution with shock

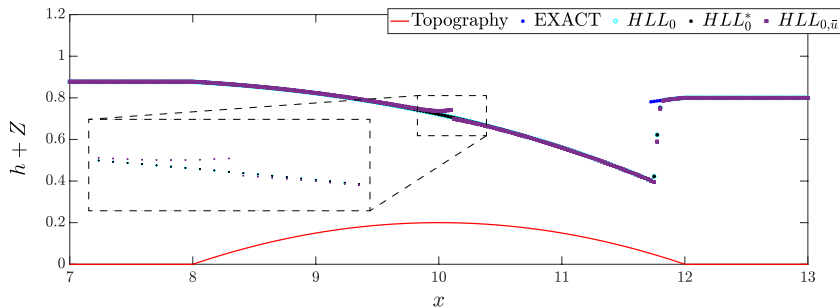


Figure – Free surface and topography for the transcritical solution with shock

| | $h + Z$ | M | S |
|-------------------|-------------|-------------|--------------|
| HLL_0 | $8.6e - 03$ | $1.9e - 03$ | $1.45e - 10$ |
| HLL_0^* | $8.6e - 03$ | $1.9e - 03$ | $1.45e - 10$ |
| $HLL_{0,\bar{u}}$ | $9.1e - 03$ | $1.8e - 03$ | $8.71e - 16$ |

Table – Free surface, discharge and shear errors for the transcritical solution with shock

One shock at left solution

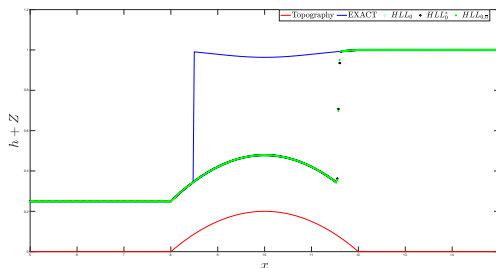


Figure – One shock at left solution for supercritical inlet and subcritical outlet boundary conditions

| | $h + Z$ | M | S |
|-------------------|-------------|-------------|--------------|
| HLL_0 | $4.5e - 03$ | $5.1e - 03$ | $2.06e - 10$ |
| HLL_0^* | $4.5e - 03$ | $5.1e - 03$ | $2.06e - 10$ |
| $HLL_{0,\bar{u}}$ | $4.7e - 03$ | $4.4e - 03$ | $2.06e - 10$ |

Table – Free surface, discharge and shear errors

Conclusion and perspectives

Conclusions

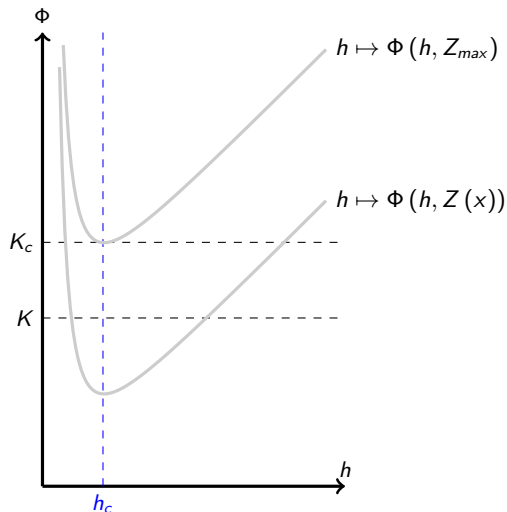
- Analysed the C^1 piecewise steady state solutions
- Proved the (Non) existence and (non) uniqueness of steady state solutions
- Constructed approximate Riemann solver for the homogeneous model and the model with topography
- Studied numerically the non-stability of the solutions with a shock at the left of the bump

Perspectives

- Understand the origin the non-entropic stationary shock obtained with the $HLL_{0,\bar{u}}$ scheme for the transcritical solutions and then try to correct it.
- Develop schemes that satisfy the dissipation of entropy.
- Study the numerical effect of the friction source term on the solutions with a shock on the left of the bump, see [Defina, Susin et Viero, 08].

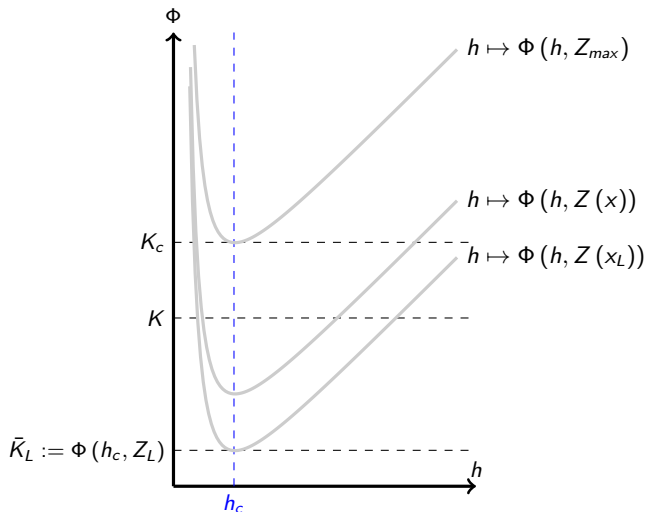
Regular moving steady states solutions

For $K < K_c$



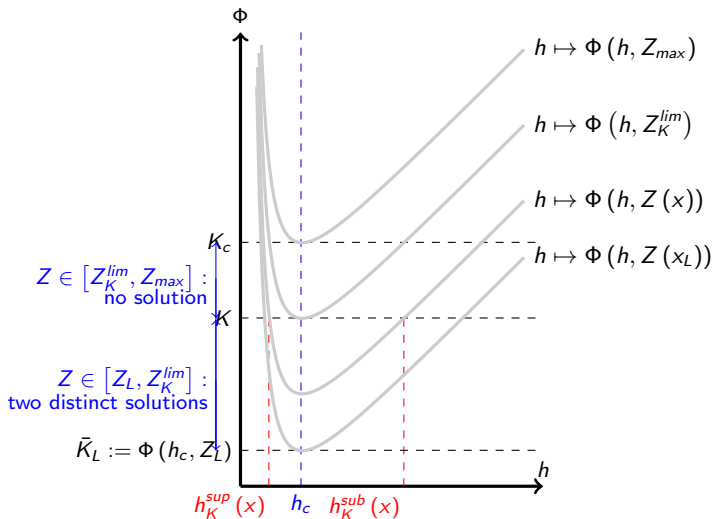
Regular moving steady states solutions

For $K < K_c$



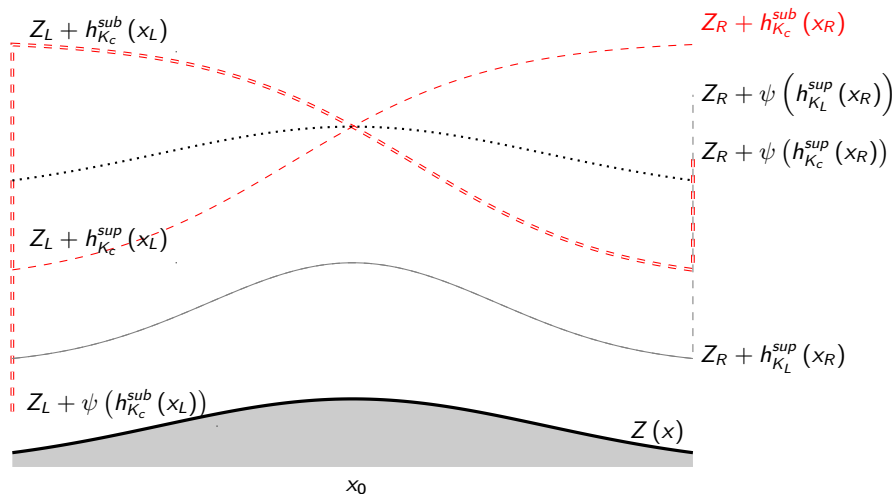
Regular moving steady states solutions

For $K < K_c$



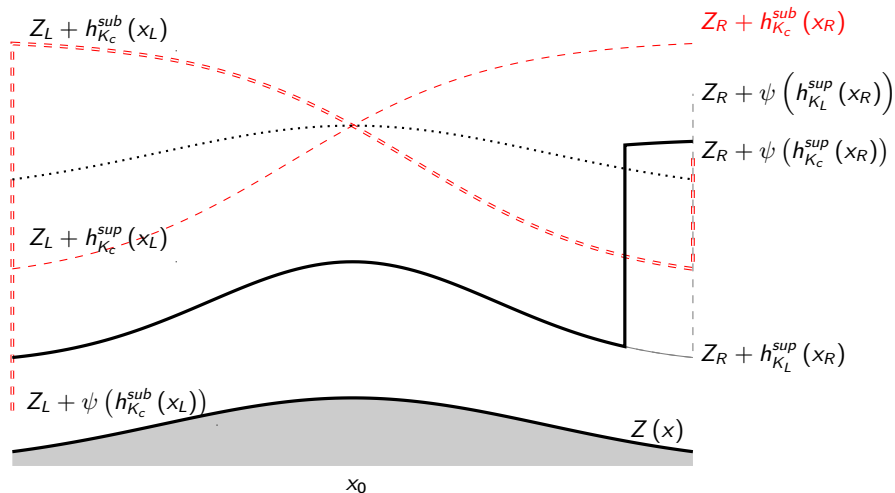
Existence

$h_L = h(x_L) < h_c$ fixed at the inlet and $h_R = h(x_R) > h_c$ fixed at the outlet



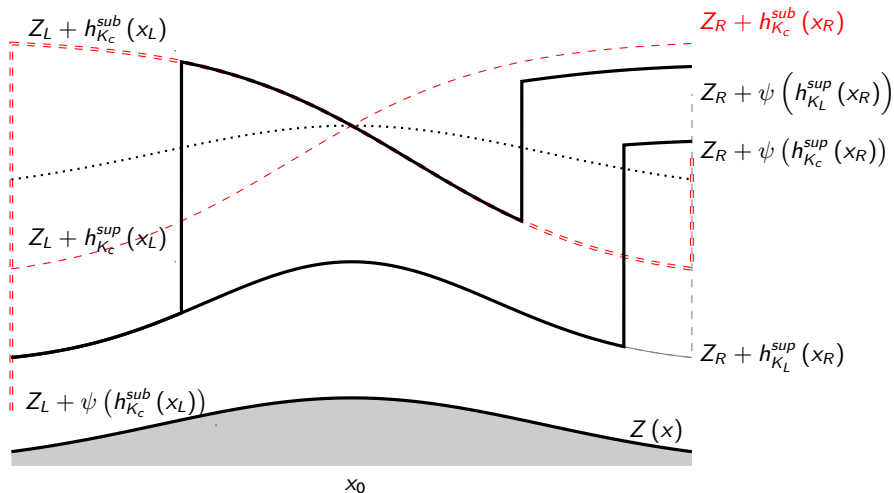
Existence

$h_L = h(x_L) < h_c$ fixed at the inlet and $h_R = h(x_R) > h_c$ fixed at the outlet



Existence

$h_L = h(x_L) < h_c$ fixed at the inlet and $h_R = h(x_R) > h_c$ fixed at the outlet



Introduction

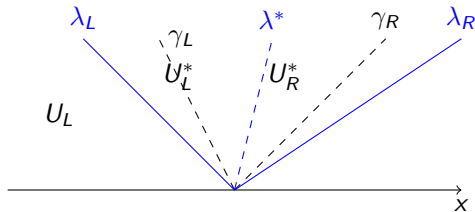
Lemma (Aguillon 18)

If $\hat{u} \neq 0$, the 2D shallow water with two velocities is strictly hyperbolic. More precisely, the eigenvalues are given by

$$\lambda_L < \gamma_L \leq \lambda^* \leq \gamma_R < \lambda_R.$$

The eigenvalues are given by

$$\left\{ \begin{array}{lcl} \lambda_L & = & \bar{u} - \sqrt{gh + 3\hat{u}^2} \\ \lambda^* & = & \bar{u}, \\ \lambda_R & = & \bar{u} + \sqrt{gh + 3\hat{u}^2}, \\ \gamma_L & = & \bar{u} - |\hat{u}|, \\ \gamma_R & = & \bar{u} + |\hat{u}|. \end{array} \right.$$



Description of the Godunov-type schemes

Finite volume framework

- We consider a uniform discretization of the computational domain
- We denote $C_i =]x_{i-\frac{1}{2}}, x_{i+\frac{1}{2}}[$ the cell of length $\Delta x = x_{i+\frac{1}{2}} - x_{i-\frac{1}{2}}$ and centered at x_i
- For any time t^n , we define $t^{n+1} = t^n + \Delta t^n$ with Δt^n satisfying a CFL condition to be described later
- Let U_i^n be a piecewise constant approximation of $U(x, t)$ at time t^n on the cell C_i
- We propose the following update formula

$$\forall i \in \mathbb{Z}, \forall n \in \mathbb{N} \quad U_i^{n+1} = U_i^n - \frac{\Delta t^n}{\Delta x} \left(\mathcal{F}_{i+\frac{1}{2}}^n - \mathcal{F}_{i-\frac{1}{2}}^n \right),$$

where

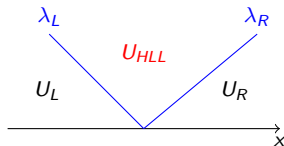
$$\mathcal{F}_{i+\frac{1}{2}}^n \approx \frac{1}{\Delta t^n} \int_{t^n}^{t^{n+1}} F \left(U \left(t, x_{i+\frac{1}{2}} \right) \right) dt.$$

The initialization of the algorithm can be computed with

$$\forall i \in \mathbb{Z} \quad U_i^0 = \frac{1}{\Delta x} \int_{x_{i-\frac{1}{2}}}^{x_{i+\frac{1}{2}}} U(x, 0) dx.$$

The *HLL* approximate Riemann solver [Lax et al, 83]

$$\tilde{U}_{HLL} \left(\frac{x}{t}, U_L, U_R \right) = \begin{cases} U_L & \text{if } \frac{x}{t} < \lambda_L, \\ U_{HLL} & \text{if } \lambda_L < \frac{x}{t} < \lambda_R, \\ U_R & \text{if } \frac{x}{t} > \lambda_R, \end{cases}$$



The consistency with the integral form of the conservation law leads to the following intermediate states

$$\begin{cases} h_{HLL} &= \frac{[h(\lambda - \bar{u})]}{[\lambda]}, \\ h_{HLL} \bar{u}_{HLL} &= \frac{[\lambda h \bar{u} - h(\bar{u}^2 + \hat{u}^2) - \frac{g}{2} h^2]}{[\lambda]}, \\ \hat{u}_{HLL} &= \frac{[\hat{u}(\lambda - \bar{u})]}{[\lambda]}. \end{cases}$$

Properties of the scheme

- Preserves the positivity of the water heights.
- Satisfies the maximum principle on S .

The *HLL* approximate Riemann solver


Discrete energy equality of the scheme

According to [Bouchut04], a scheme verifies a discrete energy inequality associated to an energy E , if there exists a numerical energy flux $\mathcal{G}(U_L, U_R)$ which is consistent with the exact energy flux, i.e $\mathcal{G}(U, U) = G(U)$ such that under some CFL condition, the discrete values computed by the scheme automatically verify

$$\forall i \in \mathbb{Z}, \forall n \in \mathbb{N}, \quad E(U_i^{n+1}) - E(U_i^n) + \frac{\Delta t^n}{\Delta x} \left(\mathcal{G}_{i+\frac{1}{2}}^n - \mathcal{G}_{i-\frac{1}{2}}^n \right) \leq 0, \quad (3)$$

where

$$\mathcal{G}_{i+\frac{1}{2}}^n = \mathcal{G}(U_{i+1}^n, U_i^n).$$

 E is a convex function of $(h, h\bar{u}, h\hat{u})$ and not $(h, h\bar{u}, \hat{u})$

The case $\hat{u}_L = \hat{u}_R = 0$: In this case the energy is convex and it was proven in [Bouchut, 04] that the *HLL* scheme verify the dissipative energy inequality.

The *HLL* approximate Riemann solver

More precisely, if (3) is verified then, it is necessarily true in the two cells. In other words, for one time step, we have

$$\left\{ \begin{array}{l} E(U_1^1) - E(U_1^0) + \frac{\Delta t^n}{\Delta x} \left(\mathcal{G}_{\frac{3}{2}}^0 - \mathcal{G}_{\frac{1}{2}}^0 \right) \leq 0, \\ E(U_2^1) - E(U_2^0) + \frac{\Delta t^n}{\Delta x} \left(\mathcal{G}_{\frac{5}{2}}^0 - \mathcal{G}_{\frac{3}{2}}^0 \right) \leq 0, \end{array} \right.$$

The *HLL* approximate Riemann solver

More precisely, if (3) is verified then, it is necessarily true in the two cells. In other words, for one time step, we have

$$\begin{cases} E(U_1^1) - E(U_1^0) + \frac{\Delta t^n}{\Delta x} \left(\mathcal{G}_{\frac{3}{2}}^0 - \mathcal{G}_{\frac{1}{2}}^0 \right) \leq 0, \\ E(U_2^1) - E(U_2^0) + \frac{\Delta t^n}{\Delta x} \left(\mathcal{G}_{\frac{5}{2}}^0 - \mathcal{G}_{\frac{3}{2}}^0 \right) \leq 0, \end{cases}$$

\Rightarrow

$$\Delta E^{0,1} := E(U_2^1) + E(U_1^1) - (E(U_2^0) + E(U_1^0)) + \frac{\Delta t^n}{\Delta x} \left(\mathcal{G}_{\frac{5}{2}}^0 - \mathcal{G}_{\frac{1}{2}}^0 \right) \leq 0. \quad (4)$$

where $\mathcal{G}_{\frac{5}{2}}^n = G(U_2^n)$ and $\mathcal{G}_{\frac{1}{2}}^n = G(U_1^n)$ due to the consistency with the exact energy flux.

The case $\hat{u}_L \neq 0$ and $\hat{u}_R \neq 0$: We conclude through the numerical results that the *HLL* scheme verifies (4). In this case, we might think that is dissipative even if it is very diffusive on the transport wave.

The *HLL* approximate Riemann solver

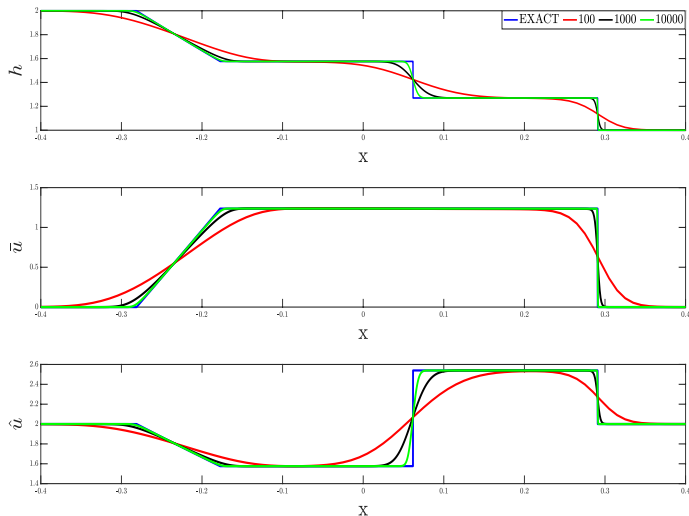


Figure – Dam Break case : Plots of the variables using the *HLL* scheme for 100, 1000 and 10000 points.

The HLL^* approximate Riemann solver

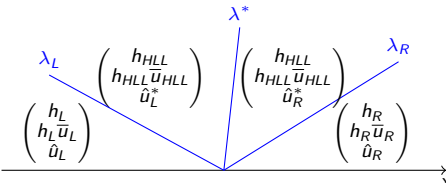
- The quantity $\frac{\hat{u}}{h}$ jumps only along the intermediate contact discontinuity. In fact, from (SW_2) , we can deduce that for regular solutions

$$\partial_t\left(\frac{\hat{u}}{h}\right) + \bar{u}\partial_x\left(\frac{\hat{u}}{h}\right) = 0.$$

- The HLL scheme is used to update only the classical shallow water variables (h, \bar{u}) and to compute the interface mass and momentum fluxes \mathcal{F}_{HLL}^h and $\mathcal{F}_{HLL}^{h\bar{u}}$.
- The shear velocity \hat{u} is updated using an upwind strategy

$$\mathcal{F}_{\{HLL, up, i+\frac{1}{2}\}}^{\hat{u}} = \frac{\hat{u}_i^n}{h_i^n} \mathcal{F}_{\{HLL, i+\frac{1}{2}\}}^{h+} + \frac{\hat{u}_{i+1}^n}{h_{i+1}^n} \mathcal{F}_{\{HLL, i+\frac{1}{2}\}}^{h-},$$

The HLL^* approximate Riemann solver

$$\tilde{U}_{HLL^*}\left(\frac{x}{t}, U_L, U_R\right) = \begin{cases} U_L & \text{if } \frac{x}{t} < \lambda_L, \\ U_L^* & \text{if } \lambda_L < \frac{x}{t} < \tilde{\lambda}, \\ U_R^* & \text{if } \tilde{\lambda} < \frac{x}{t} < \lambda_R, \\ U_R & \text{if } \frac{x}{t} > \lambda_R. \end{cases}$$


The diagram illustrates the HLL* Riemann solver in the (h, u) plane. A horizontal axis represents x . Three waves originate from the initial discontinuity at $x=0$: λ_L (left-moving), λ^* (middle), and λ_R (right-moving). The states in the (h, u) plane are represented as vectors from the origin: $\begin{pmatrix} h_L \\ h_L \bar{u}_L \\ \hat{u}_L \end{pmatrix}$ for the left state, $\begin{pmatrix} h_{HLL} \\ h_{HLL} \bar{u}_{HLL} \\ \hat{u}_L^* \end{pmatrix}$ for the intermediate state, $\begin{pmatrix} h_{HLL} \\ h_{HLL} \bar{u}_{HLL} \\ \hat{u}_R^* \end{pmatrix}$ for the other intermediate state, and $\begin{pmatrix} h_R \\ h_R \bar{u}_R \\ \hat{u}_R \end{pmatrix}$ for the right state.

To construct the numerical scheme

- 1 we consider the consistency relations
- 2 we impose the continuity of h and \bar{u} through the λ^* -wave

$$h_L^* = h_R^* \quad \text{and} \quad \bar{u}_L^* = \bar{u}_R^*.$$

- 3 we impose the continuity of $\frac{\hat{u}}{h}$ on the external waves λ_L and λ_R

$$\frac{\hat{u}_L}{h_L} = \frac{\hat{u}_L^*}{h_L^*} \quad \text{and} \quad \frac{\hat{u}_R}{h_R} = \frac{\hat{u}_R^*}{h_R^*}.$$

The HLL^* approximate Riemann solver

For $\frac{\hat{u}_R}{h_R} \neq \frac{\hat{u}_L}{h_L}$, the intermediate states are

$$\left\{ \begin{array}{l} h_L^* = h_{HLL}, \\ h_R^* = h_{HLL}, \\ \bar{u}_L^* = \bar{u}_{HLL}, \\ \bar{u}_R^* = \bar{u}_{HLL}, \\ \hat{u}_L^* = \hat{u}_L \frac{h_{HLL}}{h_L}, \\ \hat{u}_R^* = \hat{u}_R \frac{h_{HLL}}{h_R}, \\ \lambda^* = \lambda_R - \frac{h_R(\lambda_R - \bar{u}_R)}{h_{HLL}}. \end{array} \right. \quad (HLL^*)$$

If $\frac{\hat{u}_R}{h_R} = \frac{\hat{u}_L}{h_L}$, we get $\hat{u}_L^* = \hat{u}_R^* = \hat{u}_{HLL}$ and we choose λ^* defined above.
In addition, we have

- $\lambda_L < \lambda^* < \lambda_R$
- $sgn(\mathcal{F}_{\{HLL\}}^h) = sgn(\lambda^*)$
- $\mathcal{F}_{\{HLL, up\}}^{\hat{u}} = \mathcal{F}_{HLL^*}^{\hat{u}}$

The HLL^* approximate Riemann solver

Properties of the scheme

- Preserves the positivity of the water heights.
- Satisfies the maximum principle on S .
- Is not able to maintain an isolated contact discontinuity.
- Is equivalent to the HLL scheme for $\hat{u} = 0$
- Doesn't verify the discrete entropy inequality

The HLL^* approximate Riemann solver

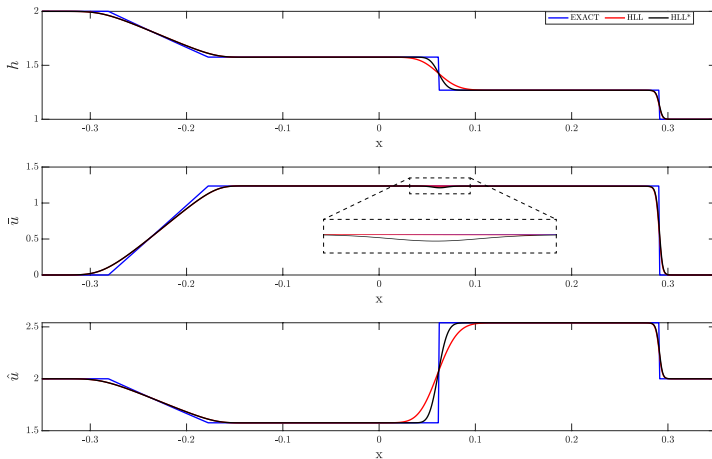


Figure – Dam Break case : Plots of the variables using the HLL and HLL^* scheme for 1000 points.

Numerical results

To ensure that the CFL condition is satisfied, we set

$$\Delta t^n = \alpha_{CFL} \frac{\Delta x}{2\Gamma} \quad , \quad \Gamma = \max_i \left(|\lambda_{L,i+\frac{1}{2}}^n|, |\lambda_{R,i+\frac{1}{2}}^n| \right)$$

with $0 < \alpha_{CFL} \leq 1$. In the following, we set $\alpha_{CFL} = 0.9$.

We compare the solutions computed by the several schemes with the analytical solution of the Riemann problems, see [Aguillon et al, 18]. In addition to that, for a domain discretized with nx cells we compute the L^2 errors using the following expression

$$L^2 = \sqrt{\frac{1}{nx} \sum_{i=1}^{nx} (U_i - U_i^{ex})^2}$$

where U_i and U_i^{ex} are respectively the approximate and the exact solutions at the cell C_i and at the physical time t_{end} .

Numerical results

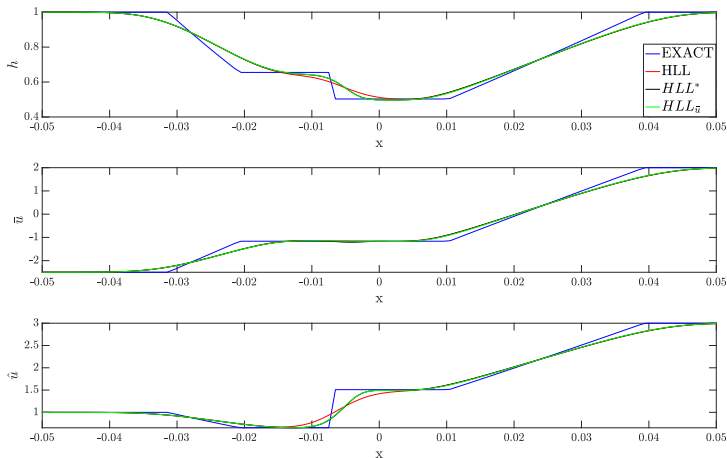


Figure – The two rarefactions case. Plots of the variables using HLL , HLL^* and $HLL_{\bar{u}}$ solvers for 1000 grid cells

Numerical results

| nx | err_{HLL} | $order_{HLL}$ | err_{HLL}^* | $order_{HLL}^*$ | $err_{HLL_{\overline{U}}}$ | $order_{HLL_{\overline{U}}}$ |
|--------|-------------|---------------|---------------|-----------------|----------------------------|------------------------------|
| 10^2 | 3.6e-02 | - | 3.8e-012 | - | 3.8e-02 | - |
| 10^3 | 1.1e-02 | 0.56 | 9.7e-03 | 0.59 | 9.6e-03 | 0.59 |
| 10^4 | 3.3e-03 | 0.47 | 2.9e-03 | 0.51 | 2.9e-03 | 0.51 |
| 10^5 | 1.5e-03 | 0.34 | 1.2e-03 | 0.39 | 1.2e-03 | 0.39 |
| 10^6 | 8e-04 | 0.26 | 6e-04 | 0.28 | 6e-04 | 0.28 |

Table – Height error and order of accuracy for the two rarefactions problem

| nx | err_{HLL} | $order_{HLL}$ | err_{HLL}^* | $order_{HLL}^*$ | $err_{HLL_{\overline{U}}}$ | $order_{HLL_{\overline{U}}}$ |
|--------|-------------|---------------|---------------|-----------------|----------------------------|------------------------------|
| 10^2 | 1.6e-01 | - | 1.6e-01 | - | 1.6e-01 | - |
| 10^3 | 4.4e-02 | 0.57 | 4.4e-02 | 0.55 | 4.3e-02 | 0.56 |
| 10^4 | 1e-02 | 0.63 | 1e-02 | 0.63 | 1e-02 | 0.62 |
| 10^5 | 2.1e-03 | 0.7 | 2e-03 | 0.7 | 2e-03 | 0.69 |
| 10^6 | 3e-04 | 0.73 | 3e-04 | 0.73 | 4e-04 | 0.73 |

Table – Mean velocity error and order of accuracy for the two rarefactions problem

| nx | err_{HLL} | $order_{HLL}$ | err_{HLL}^* | $order_{HLL}^*$ | $err_{HLL_{\overline{U}}}$ | $order_{HLL_{\overline{U}}}$ |
|--------|-------------|---------------|---------------|-----------------|----------------------------|------------------------------|
| 10^2 | 1.1e-01 | - | 1.1e-01 | - | 1.1e-01 | - |
| 10^3 | 3.3e-02 | 0.49 | 3.1e-02 | 0.55 | 3e-02 | 0.55 |
| 10^4 | 1.5e-02 | 0.35 | 1.2e-02 | 0.41 | 1.2e-02 | 0.41 |
| 10^5 | 8e-03 | 0.26 | 6e-03 | 0.27 | 6e-03 | 0.27 |
| 10^6 | 4e-03 | 0.25 | 3e-03 | 0.25 | 3.5e-03 | 0.25 |

Table – Standard deviation error and order of accuracy for the two rarefactions problem

Numerical results

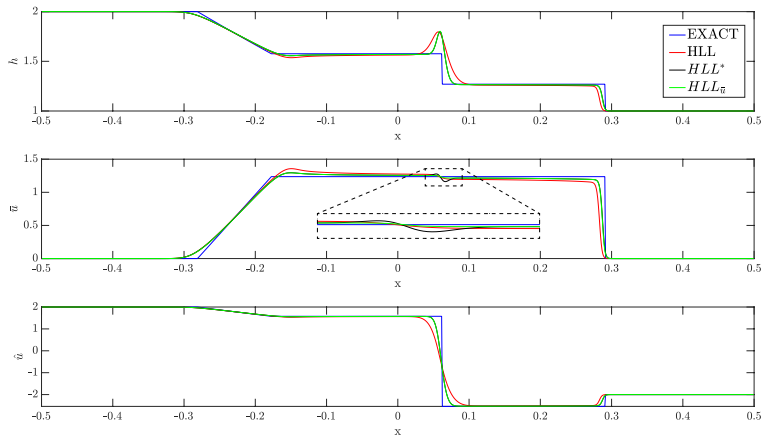


Figure – Dam break problem with change of sign on \hat{u} . Plots of the variables using HLL , HLL^* and $HLL_{\bar{u}}$ solvers for 1000 grid cells

Numerical results

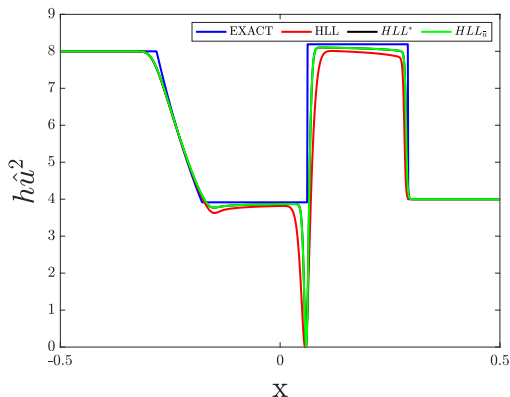


Figure – Dam break problem with change of sign on \hat{u} . Plots of the $h\hat{u}^2$ using HLL , HLL^* and $HLL_{\bar{u}}$ solvers for 1000 grid cells

Numerical results

| nx | err_{HLL} | $order_{HLL}$ | err_{HLL}^* | $order_{HLL}^*$ | $err_{HLL_{\overline{u}}}$ | $order_{HLL_{\overline{u}}}$ |
|--------|-------------|---------------|---------------|-----------------|----------------------------|------------------------------|
| 10^2 | 8.8e-02 | - | 6.6e-02 | - | 6.8e-02 | - |
| 10^3 | 5.3e-02 | 0.24 | 3.8e-02 | 0.3 | 3.8e-02 | 0.31 |
| 10^4 | 3.1e-02 | 0.24 | 2.2e-02 | 0.24 | 2.2e-02 | 0.24 |
| 10^5 | 1.7e-02 | 0.24 | 1.2e-02 | 0.24 | 1.2e-02 | 0.24 |
| 10^6 | 9e-03 | 0.25 | 7e-03 | 0.25 | 7e-03 | 0.25 |

Table – Height error and order of accuracy for the Dam break problem with change of sign on \hat{u}

| nx | err_{HLL} | $order_{HLL}$ | err_{HLL}^* | $order_{HLL}^*$ | $err_{HLL_{\overline{u}}}$ | $order_{HLL_{\overline{u}}}$ |
|--------|-------------|---------------|---------------|-----------------|----------------------------|------------------------------|
| 10^2 | 2e-01 | - | 1.4e-01 | - | 1.4e-01 | - |
| 10^3 | 1e-01 | 0.23 | 5e-02 | 0.32 | 6e-02 | 0.29 |
| 10^4 | 6e-02 | 0.21 | 4.2e-02 | 0.2 | 4e-02 | 0.21 |
| 10^5 | 3e-02 | 0.24 | 2.4e-02 | 0.22 | 2.5e-02 | 0.22 |
| 10^6 | 2e-02 | 0.24 | 1.4e-02 | 0.24 | 1.4e-02 | 0.24 |

Table – Mean velocity error and order of accuracy for the Dam break problem with change of sign on \hat{u}

| nx | err_{HLL} | $order_{HLL}$ | err_{HLL}^* | $order_{HLL}^*$ | $err_{HLL_{\overline{u}}}$ | $order_{HLL_{\overline{u}}}$ |
|--------|-------------|---------------|---------------|-----------------|----------------------------|------------------------------|
| 10^2 | 4.1e-01 | - | 2.8e-01 | - | 2.9e-01 | - |
| 10^3 | 2.3e-01 | 0.24 | 1.6e-01 | 0.31 | 1.6e-01 | 0.3 |
| 10^4 | 1.3e-01 | 0.25 | 9e-02 | 0.25 | 9e-02 | 0.24 |
| 10^5 | 7e-02 | 0.24 | 5e-02 | 0.24 | 5e-02 | 0.24 |
| 10^6 | 4e-02 | 0.24 | 2e-02 | 0.24 | 2.e-02 | 0.24 |

Table – Standard deviation error and order of accuracy for the Dam break problem with change of sign on \hat{u}

The main objective of this work is to derive numerical schemes that

- ❶ preserve the positivity of the water height
- ❷ preserve the maximum principle on $S = \frac{\hat{u}}{h}$
- ❸ are accurate for the transport process associated to the shear velocity
- ❹ are accurate on the contact discontinuity while verifying a well-balanced property for all regular steady states of the system (SW_2).

To do so we

- approximate the source term
- we extend the numerical schemes constructed for the homogeneous model to adapt with the presence of the stationary wave

Steady states solutions

The C^1 steady states of (SW_2) system are governed by

$$\begin{cases} \partial_x(h\bar{u}) = 0, \\ \partial_x(h(\bar{u}^2 + \hat{u}^2) + \frac{g}{2}h^2) = -gh\partial_x Z, \\ \partial_x(\bar{u}\hat{u}) = 0 \end{cases} \implies \begin{cases} h\bar{u} = M, \\ \frac{\bar{u}^2}{2} + \frac{3\hat{u}^2}{2} + g(h + Z) = K, \\ \bar{u}\hat{u} = MS. \end{cases}$$

For all $W_L = (h_L, h_L\bar{u}_L, \hat{u}_L, Z_L)$ and $W_R = (h_R, h_R\bar{u}_R, \hat{u}_R, Z_R)$ at steady state, the well balanced approximate Riemann solver \tilde{W} should verify

$$\tilde{W}\left(\frac{x}{t}, W_L, W_R\right) = \begin{cases} W_L & \text{if } \frac{x}{t} < 0, \\ W_R & \text{if } \frac{x}{t} > 0. \end{cases}$$

Let us introduce the quantity (steady state indicator introduced first by [Berthon et al, 21])

$$\epsilon_{L,R} = |K_R - K_L| + |M_R - M_L| + |S_R - S_L|.$$

The smooth steady state solutions of (SW_2) for a Riemann problem are then characterized by

$$\epsilon_{L,R} = 0.$$

Proposition

Suppose that $W_L = (U_L, Z_L)$ and $W_R = (U_R, Z_R)$ define a smooth steady state solution . The approximation of the topography source term ensures the relation

$$\Delta x \cdot \tilde{B}^M = M^2 \left[\frac{1}{h} \right]_L^R + S^2 [h^3]_L^R + \frac{g}{2} [h^2]_L^R .$$

which is a discrete version of the second equation of the regular steady state solutions.

The approximation of the source term

- ensures the relation

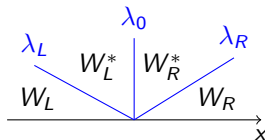
$$\Delta x \cdot \tilde{B}^M = M^2 \left[\frac{1}{h} \right]_L^R + S^2 [h^3]_L^R + \frac{g}{2} [h^2]_L^R .$$

which is a discrete version of the second equation of the regular steady state solutions for $W_L = (U_L, Z_L)$ and $W_R = (U_R, Z_R)$ defining a smooth steady state solution

- is ill-defined if $\tilde{F}_{\tilde{h}, M, S} = 1$ and $\epsilon_{L,R} = 0$. Then, as in [Berthon, 21], we choose

The HLL_0 scheme

This approximate Riemann solver is an extension of the HLL scheme to take into consideration the stationary wave. This solver is similar to the scheme initially proposed for the shallow water equations with topography in [Berthon et al, 16].



- In this scheme and in this work we choose to impose that the topography is only discontinuous on the stationary wave, i.e $Z_L^* = Z_L$ and $Z_R^* = Z_R$.
- We have six unknowns : $W_L^* = (h_L^*, h_L^* \bar{u}_L^*, \hat{u}_L^*)$ and $W_R^* = (h_R^*, h_R^* \bar{u}_R^*, \hat{u}_R^*)$.

The HLL_0 scheme

We consider a linearization as done in [Berthon et al, 21]

$$\left(\frac{-\overline{M^2}}{h_L h_R} + \frac{g}{2} (h_R + h_L) + \overline{S^2} (h_R^2 + h_L h_R + h_L^2) \right) (h_R^* - h_L^*) = \Delta x \cdot \tilde{B}.$$

or equivalently

$$\alpha_{L,R} (h_R^* - h_L^*) = \Delta x \cdot \tilde{B}, \quad \text{where} \quad \alpha_{L,R} = \frac{-\overline{M^2}}{h_L h_R} + \frac{g}{2} (h_R + h_L) + \overline{S^2} (h_R^2 + h_L h_R + h_L^2).$$

So, for $\alpha_{L,R} \neq 0$ or $\epsilon_{L,R} \neq 0$ the above relation is replaced by

$$(\alpha_{L,R}^2 + \epsilon_{L,R}) (h_R^* - h_L^*) = \alpha_{L,R} \Delta x \cdot \tilde{B}.$$

and we define

$$C_{\alpha_{L,R}, \tilde{B}} := \frac{\alpha_{L,R} \Delta x \cdot \tilde{B}}{\alpha_{L,R}^2 + \epsilon_{L,R}}.$$

Then, the sixth relation is

$$(h_R^* - h_L^*) = C_{\alpha_{L,R}, \tilde{B}}.$$

⚠ When $\alpha_{L,R} = \epsilon_{L,R} = 0$ we choose to impose

$$(h_R^* - h_L^*) = (h_R - h_L).$$

The HLL_0 scheme

The linearization (24) is ill-posed for $\alpha_{L,R} = \epsilon_{L,R} = 0$. After straight forward computations, we get

$$\lim_{\alpha_{L,R} \rightarrow 0} \lim_{\epsilon_{L,R} \rightarrow 0} \frac{\alpha_{L,R} \Delta x \cdot \tilde{B}}{(\alpha_{L,R}^2 + \epsilon_{L,R})} = h_R - h_L,$$

but

$$\lim_{\epsilon_{L,R} \rightarrow 0} \lim_{\alpha_{L,R} \rightarrow 0} \frac{\alpha_{L,R} \Delta x \cdot \tilde{B}}{(\alpha_{L,R}^2 + \epsilon_{L,R})} = 0.$$

Here, as in [?], when $\alpha_{L,R} = \epsilon_{L,R} = 0$ we choose to impose

$$(h_R^* - h_L^*) = (h_R - h_L).$$

The HLL_0 scheme

Other correction strategies

The strategy proposed by [Audusse et al, 15] consists on

- setting the intermediate water height and the standard deviation to zero

$$\begin{cases} h_{k*} = 0, \\ M_{k*} = M^*, \\ \hat{u}_{k*} = 0 \end{cases}$$

where k corresponds to L or R depending on the state of the negative quantity.

The strategy proposed by [Berthon et al, 21] consists on

- introducing a parameter γ such that

$$0 \leq \gamma \leq \min(h_L, h_R, h_{HLL}).$$

- setting $h_{k*} = \gamma$ and to consider the consistency relations and the first and third equilibrium relation.

The HLL_0^* approximated Riemann solver

- 1 A first possibility is to construct a HLL_0^* solver using an upwind strategy.
- 2 A second possibility is to interpret the scheme as a four waves ARS.

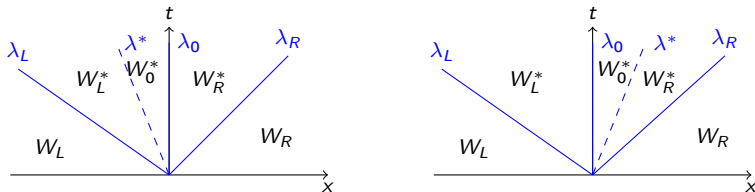


Figure – The waves representation of the HLL_0^* approximate Riemann solver with $\lambda^* < 0$ on the left and $\lambda^* > 0$ on the right.

The HLL_0^* approximated Riemann solver

- We consider the consistency relation
- Similarly to HLL_0 , we consider the Riemann invariant across the stationary wave

$$(h_0^* \bar{u}_0^*, \bar{u}_0^* \hat{u}_0^*) = \begin{cases} (h_R^* \bar{u}_R^*, \bar{u}_R^* \hat{u}_R^*) & \text{if } \lambda^* < 0, \\ (h_L^* \bar{u}_L^*, \bar{u}_L^* \hat{u}_L^*) & \text{if } \lambda^* > 0 \end{cases}$$

- The linearization across the stationary wave implies

$$C_{\alpha_{L,R}, \tilde{B}} = \begin{cases} (h_R^* - h_0^*) & \text{if } \lambda^* < 0, \\ (h_0^* - h_L^*) & \text{if } \lambda^* > 0 \end{cases}$$

- Similarly to HLL^* , we impose the continuity of h and \bar{u} across the transport wave.

$$(h_0^*, \bar{u}_0^*) = \begin{cases} (h_L^*, \bar{u}_L^*) & \text{if } \lambda^* < 0, \\ (h_R^*, \bar{u}_R^*) & \text{if } \lambda^* > 0 \end{cases}$$

- We impose the continuity of $\frac{\hat{u}}{h}$ on the external waves λ_L and λ_R

$$\frac{\hat{u}_L}{h_L} = \frac{\hat{u}_L^*}{h_L^*} \quad \text{and} \quad \frac{\hat{u}_R}{h_R} = \frac{\hat{u}_R^*}{h_R^*}.$$

The HLL_0^* scheme

Well-balanced version of the HLL_0^* scheme

Assume that h_L and h_R are positive. For $\frac{\hat{u}_R}{h_R} \neq \frac{\hat{u}_L}{h_L}$, the left and right intermediate states are given by

$$\left\{ \begin{array}{l} h_L^* = h_{HLL} - \frac{\lambda_R C_{\alpha_L, R, \tilde{B}}}{(\lambda_R - \lambda_L)}, \\ h_R^* = h_{HLL} - \frac{\lambda_L C_{\alpha_L, R, \tilde{B}}}{(\lambda_R - \lambda_L)}, \\ \bar{u}_L^* = \frac{h_{HLL} \bar{u}_{HLL} + \frac{\Delta x \cdot \tilde{B}}{\lambda_R - \lambda_L}}{h_L^*}, \\ \bar{u}_R^* = \frac{h_{HLL} \bar{u}_{HLL} + \frac{\Delta x \cdot \tilde{B}}{\lambda_R - \lambda_L}}{h_R^*}, \\ \hat{u}_L^* = \frac{\hat{u}_L}{h_L} h_L^*, \\ \hat{u}_R^* = \frac{\hat{u}_R}{h_R} h_R^*, \end{array} \right. \quad (HLL_0^*)$$

The HLL_0^* scheme

Well-balanced version of the HLL_0^* scheme

Assume that $h_L^* > 0$ and $h_R^* > 0$.

- Suppose $\lambda^* > 0$ then,

$$\lambda^* = \frac{\lambda_R h_R^* - h_R (\lambda_R - \bar{u}_R)}{h_R^*} > 0 \Leftrightarrow \lambda_R h_R^* - h_R (\lambda_R - \bar{u}_R) > 0,$$

- Suppose $\lambda^* < 0$ then,

$$\lambda^* = \frac{\lambda_L h_L^* - h_L (\lambda_L - \bar{u}_L)}{h_L^*} < 0 \Leftrightarrow \lambda_L h_L^* - h_L (\lambda_L - \bar{u}_L) < 0,$$

But, the consistency relation on the water height implies

$$\lambda_L h_L^* - \lambda_L h_L + \bar{u}_L h_L = \lambda_R h_R^* - \lambda_R h_R + \bar{u}_R h_R.$$

The HLL_0^* scheme

Well-balanced version of the HLL_0^* scheme

Assume that $h_L^* > 0$ and $h_R^* > 0$.

- Suppose $\lambda^* > 0$ then,

$$\lambda^* = \frac{\lambda_R h_R^* - h_R (\lambda_R - \bar{u}_R)}{h_R^*} > 0 \Leftrightarrow \lambda_R h_R^* - h_R (\lambda_R - \bar{u}_R) > 0,$$

- Suppose $\lambda^* < 0$ then,

$$\lambda^* = \frac{\lambda_L h_L^* - h_L (\lambda_L - \bar{u}_L)}{h_L^*} < 0 \Leftrightarrow \lambda_L h_L^* - h_L (\lambda_L - \bar{u}_L) < 0,$$

But, the consistency relation on the water height implies

$$\textcolor{red}{I} := \lambda_L h_L^* - \lambda_L h_L + \bar{u}_L h_L = \lambda_R h_R^* - \lambda_R h_R + \bar{u}_R h_R.$$

The HLL_0^* scheme

Well-balanced version of the HLL_0^* scheme

And we impose

$$\lambda^* = \begin{cases} \frac{I}{h_R^*} & \text{if } I > 0, \\ \frac{I}{h_L^*} & \text{if } I < 0 \end{cases}$$

that satisfies

$$\lambda_L < \lambda^* < \lambda_R.$$

Assume that h_L and h_R are positive and $\frac{\hat{u}_R}{h_R} \neq \frac{\hat{u}_L}{h_L}$. The intermediate state W_0^* is given by

If $\lambda^* > 0$

If $\lambda^* < 0$

$$\begin{cases} h_0^* = h_{HLL} - \frac{\lambda_L C_{\alpha_L, R, \tilde{B}}}{(\lambda_R - \lambda_L)}, \\ \bar{u}_0^* = \frac{h_{HLL} \bar{u}_{HLL} + \frac{\Delta x \cdot \tilde{B}}{\lambda_R - \lambda_L}}{h_0^*}, \\ \hat{u}_0^* = \frac{\hat{u}_L}{h_L} h_0^*, \end{cases}$$

$$\begin{cases} h_0^* = h_{HLL} - \frac{\lambda_R C_{\alpha_L, R, \tilde{B}}}{(\lambda_R - \lambda_L)}, \\ \bar{u}_0^* = \frac{h_{HLL} \bar{u}_{HLL} + \frac{\Delta x \cdot \tilde{B}}{\lambda_R - \lambda_L}}{h_0^*}, \\ \hat{u}_0^* = \frac{\hat{u}_R}{h_R} h_0^*. \end{cases}$$

Assume that h_L and h_R are positive. For W_L and W_R defining a smooth steady state the intermediate states satisfy the well-balanced property.

Positive and well-balanced version of the HLL_0^* scheme

According

$$(h_0^*, \bar{u}_0^*) = \begin{cases} (h_L^*, \bar{u}_L^*) & \text{if } \lambda^* < 0, \\ (h_R^*, \bar{u}_R^*) & \text{if } \lambda^* > 0 \end{cases}$$

and

$$\lambda_R h_R^* - \lambda_L h_L^* = (\lambda_R - \lambda_L) h_{HLL},$$

we can conclude that only one quantity among h_L^* or h_R^* can be negative. More precisely, if $h_L^* < 0$ then,

$$h_R^* > 0 \implies I > 0 \implies \lambda^* > 0 \implies h_0^* = h_R^* > 0,$$

and if $h_R^* < 0$ then,

$$h_L^* > 0 \implies I < 0 \implies \lambda^* < 0 \implies h_0^* = h_L^* > 0.$$

Positive and well-balanced version of the HLL_0^* scheme

To ensure the positivity of all intermediate water heights we will test the sign of

$$\tilde{h}_L^* = h_{HLL} - \frac{\lambda_R C_{\alpha_L, R, \tilde{B}}}{(\lambda_R - \lambda_L)} \quad \text{and} \quad \tilde{h}_R^* = h_{HLL} - \frac{\lambda_L C_{\alpha_L, R, \tilde{B}}}{(\lambda_R - \lambda_L)}.$$

- The case $\tilde{h}_L^* > 0$ and $\tilde{h}_R^* > 0$ then, the intermediate states defined earlier
- The case $\tilde{h}_L^* < 0$ and $\tilde{h}_R^* > 0$ then, we replace the equilibrium relations by the fact that the L^* intermediate state vanishes
- The case $\tilde{h}_L^* > 0$ and $\tilde{h}_R^* < 0$ then, the equilibrium relations are replaced by the fact that R^* intermediate states vanishes

$$\begin{cases} h_L^* = 0, \\ \bar{u}_L^* = 0, \\ \hat{u}_L^* = 0, \end{cases}$$

$$\begin{cases} h_R^* = 0, \\ \bar{u}_R^* = 0, \\ \hat{u}_R^* = 0, \end{cases}$$

In each case we show that $\lambda_L < \lambda^* < \lambda_R$